

AD-A037 104

VIRGINIA POLYTECHNIC INST AND STATE UNIV BLACKSPURG --ETC F/G 11/9
THE WEAR OF POLYMERS BY TRANSFERRED FILMS.(U)
JAN 77 N S EISS

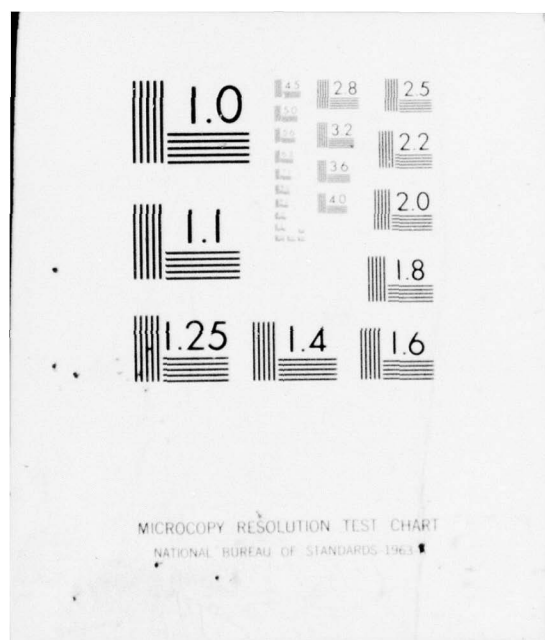
UNCLASSIFIED

ARO-11229.3-E

DA-ARO-D-31-124-73-G170
NL

1 OF 2
AD
A037104



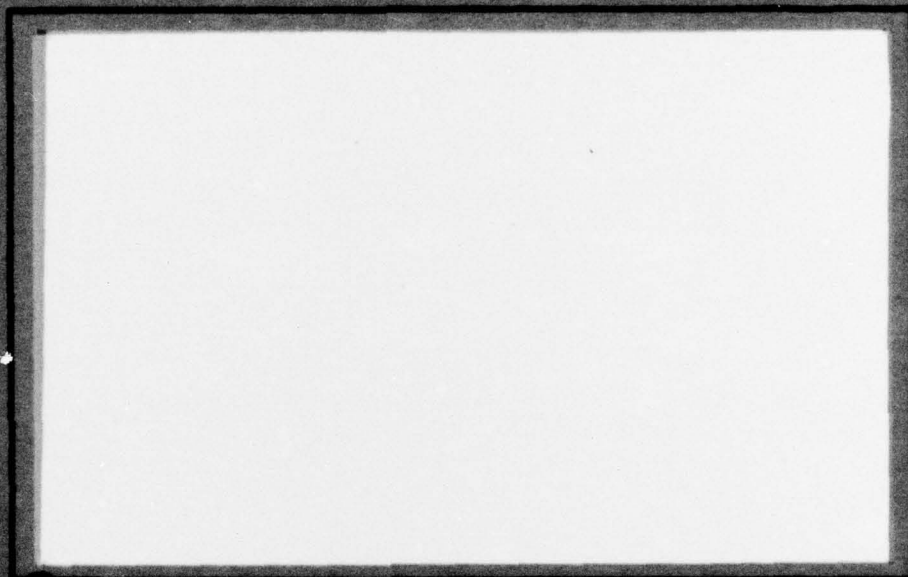


QRO. 11229. 3-E✓

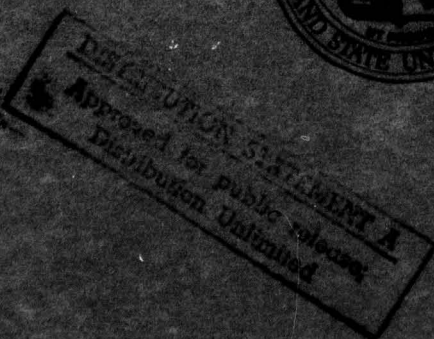
12
B. S.

ADA 037104

OF **COLLEGE
ENGINEERING**



**VIRGINIA
POLYTECHNIC
INSTITUTE
AND
STATE
UNIVERSITY**



The findings in this report are not
official Department of the Army position, unless
designated by other authorized documents.

**BLACKSBURG,
VIRGINIA**

12

THE WEAR OF POLYMERS BY TRANSFERRED FILMS

FINAL REPORT

NORMAN S. EISS, JR.

ASSOCIATE PROFESSOR MECHANICAL ENGINEERING

15 JANUARY 1977

U. S. ARMY RESEARCH OFFICE

GRANT NUMBERS

DA-ARO-D-31-124-73-G170

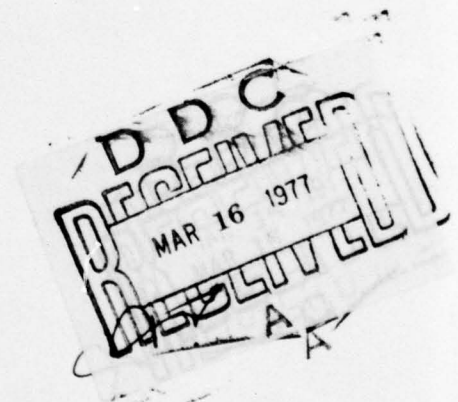
DAHCO4-75-G-0008

DAAG29-76-G-0009

VIRGINIA POLYTECHNIC INSTITUTE AND STATE UNIVERSITY

BLACKSBURG, VIRGINIA

APPROVED FOR PUBLIC RELEASE DISTRIBUTION UNLIMITED



Security Classification

DOCUMENT CONTROL DATA - R & D

(Security classification of title, body of abstract and indexing annotation must be entered when the overall report is classified)

1. ORIGINATING ACTIVITY (Corporate author) Research Division <i>use Coll. of Eng. 406822</i> Virginia Polytechnic Institute and State University Blacksburg, Virginia 24061		2a. REPORT SECURITY CLASSIFICATION unclassified	
		2b. GROUP NA	
3. REPORT TITLE The Wear of Polymers by Transferred Films.			
4. DESCRIPTIVE NOTES (Type of report and inclusive dates) Final Report. 1 Sep 73 - 30 Nov 76.			
5. AUTHOR(S) (First name, middle initial, last name) Norman S. Eiss, Jr. <i>(12) 118p.</i>			
6. REPORT DATE 15 Jan 77		7a. TOTAL NO. OF PAGES 103	7b. NO. OF REFS 49
8. CONTRACT OR GRANT NO. a. DA-ARO-D-31-124-73-G170 <i>New</i> b. XXXXXXXX c. DAHC04-75-G-0008 d. DAAG29-76-G-0009		9a. ORIGINATOR'S REPORT NUMBER(S) None <i>(12) ARO</i>	
		9b. OTHER REPORT NO(S) (Any other numbers that may be associated with this report) None <i>(19) 11229, 3-E</i>	
10. DISTRIBUTION STATEMENT Approved for public release; distribution unlimited			
11. SUPPLEMENTARY NOTES None		12. SPONSORING MILITARY ACTIVITY U. S. Army Research Office <i>micromam</i> P. O. Box 12211 Research Triangle Park, N.C. 27709	
13. ABSTRACT A wear measuring technique was developed using radioactive tracers. The technique was capable of detecting less than 1 μg of polymer transferred to a steel surface. The technique was used to measure the wear of PCTFE and PVC in sliding experiments at sliding speeds of less than 1 cm/sec by detecting the ^{38}Cl isotope which had been made radioactive by neutron bombardment. Low density polyethylene was doped with one percent Dy_2O_3 , and the wear measured by tracing the ^{165}Dy isotope. <i>CL 38</i> Scanning electron microscope observations of the wear process showed that transfer of polymer occurred at the highest asperities on the steel surface. The transferred polymer had sheared off at an angle and the shear angles were significantly different for different polymers. For example, PCTFE, PVC, and nylon 6/6 had shear angles of 12.4, 10.9, and 19.0 degrees, respectively. The amount of polymer transfer for repeated passes over the same surface was shown to be a function of the angle that the sliding direction made with the lay on the surface. The amount of transfer was least when sliding parallel to the lay, intermediate when sliding perpendicular to the lay, and highest at angles between 10 and 80 degrees. The highest wear resulted from transferred polymer being continually moved to the edge of the wear track on subsequent passes. \rightarrow <i>DY165</i> (continued on attached sheet)			

DD FORM 1473

REPLACES DD FORM 1473, 1 JAN 64, WHICH IS OBSOLETE FOR ARMY USE.

1

Security Classification

406822

AB+

Security Classification

14. KEY WORDS	LINK A		LINK B		LINK C	
	ROLE	WT	ROLE	WT	ROLE	WT
Polymers						
Plastics						
Wear, Abrasive Wear, Wear Models						
Radiotracers						
Neutron Activation Analysis						
Polychlorotrifluoroethylene						
Polyvinyl Chloride						
Polyethylene						
Nylon 6/6						
Surface Roughness						
Surface Topography						
Transferred Films						
Orthogonal Machining Theory						
Shear Plane						
Flow Pressure						
Energy-to-Rupture						

Security Classification

13. ABSTRACT (continued)

Wear models were proposed for full penetration of the steel surface into the polymer pin (apparent and real areas approximately equal) and partial penetration (apparent area larger than real area). For full penetration, the wear model is based on orthogonal machining theory which predicts the angular location of the plane of maximum shear stress in the chip forming process. While the model could predict the relative wear of PVC and PCTFE, it predicted that asperity slopes necessary to cause shear stresses high enough for polymer fracture were larger than those measured on the surfaces. The partial penetration model was based on penetration depth and shear angle. It correctly predicted relative wear for PVC and PCTFE. The wear model and experiments emphasized the importance of complete surface topography characterization and polymer properties measured under conditions similar to those existing in sliding.

14. KEYWORDS

Polymers
Plastics
Wear, Abrasive Wear, Wear Models
Radiotracers
Neutron Activation Analysis
Polychlorotrifluoroethylene
Polyvinyl Chloride
Polyethylene
Nylon 6/6
Surface Roughness
Surface Topography
Transferred Films
Orthogonal Machining Theory
Shear Plane
Flow Pressure
Energy-to-Rupture

ACCESSION for	
NTIS	White Section <input checked="" type="checkbox"/>
DIC	Buff Section <input type="checkbox"/>
UNANNOUNCED	<input type="checkbox"/>
JUSTIFICATION	
BY	
DISTRIBUTION/AVAILABILITY CODES	
Dist.	AVAIL. and/or SPECIAL
A	

Personnel

The following personnel were supported by these grants:

Norman S. Eiss, Jr., Associate Professor, Mechanical Engineering, VPI&SU,
Principal Investigator.

Terrance F. J. Quinn, Visiting Professor of Mechanical Engineering, VPI&SU
(currently University of Aston, Birmingham, England).

Stephen D. Doolittle, Graduate Research Assistant, Mechanical Engineering,
VPI&SU, M.S. degree, 1974. (currently Disston, Inc., Danville, Va.)

Jeffery H. Warren, Graduate Research Assistant, Mechanical Engineering, VPI&SU,
Ph.D. degree, 1976. (currently Dupont Savannah River Laboratory, Aiken,
South Carolina)

The experimental work for the theses of the following students was
supported by these grants.

Gary D. Lerch, Mechanical Engineering, VPI&SU, M.S. degree, 1974. (currently
1st Lt. U.S. Army, stationed in Germany)

Kathryn C. Wood, Mechanical Engineering, VPI&SU, M.S. degree, 1976. (currently
Westinghouse Corp., Pittsburgh, Pa.)

Publications

- Eiss, N. S., Jr. and J. H. Warren, "The Effect of Surface Finish on the Friction and Wear of PCTFE Plastic on Mild Steel," Soc. Mfg. Eng. Paper No. IQ7S-125 (April 1975).
- Eiss, N. S., Jr., S. D. Doolittle, and J. H. Warren, "An Application of Neutron Activation Analysis to the Measurement of the Wear of Polymers," Wear, 38 (1976) 125-139.
- Eiss, N. S., Jr., J. H. Warren, and T. F. J. Quinn, "On the Influence of the Degree of Crystallinity of PCTFE on its Transfer to Steel Surfaces of Different Roughnesses," presented at the Leeds-Lyon Symposium on the Friction and Wear of Non-Metallic Materials, 7-10 September 1976, Leeds, England.
- Warren, J. H. and N. S. Eiss, Jr. "Depth of Penetration as a Predictor of the Wear of Polymers on Hard Rough Surfaces," accepted for presentation and publication in proceedings of the Conference on Wear of Materials, St. Louis, Mo., April 26-28, 1977.

Theses, Dissertations

- Lerch, Gary D., "A Scanning Electron Microscope Study of the Wear of Polychlorotrifluoroethylene on Steel," M.S. Thesis, VPI&SU, August 1974.
- Doolittle, Stephen D., "A Radio-tracer Study of the Effect of Surface Finish on the Transfer of Polychlorotrifluoroethylene Sliding on Mild Steel," M.S. thesis, VPI&SU, August 1974.
- Wood, Kathryn C., "A Study of the Addition of a Radio-Tracer Agent to Polyethylene for the Measurement of Wear Using Neutron Activation Analysis," M.S. Thesis, VPI&SU, August 1976.

Warren, J. H., "The Prediction of Polymer Wear Using Polymer Mechanical Properties and Surface Characterization Parameters," Ph.D. dissertation, VPI&SU, August 1976.

TABLE OF CONTENTS

	Page
ABSTRACT	i
Personnel	iii
Publications, Theses, and Dissertations	iv
LIST OF FIGURES	vii
LIST OF TABLES	ix
1. INTRODUCTION	1
2. SUMMARY	4
2.1 Wear Measurement by Neutron Activation Analysis (NAA)	4
2.2 Observations in the Scanning Electron Microscope (SEM)	5
2.3 Wear Model Development	5
3. DISCUSSION	8
3.1 Wear Measurement by Neutron Activation Analysis (NAA)	8
3.2 Scanning Electron Microscope Observations	12
3.3 Wear Model Development	19
4. REFERENCES	24
APPENDICES	
1. The Effect of Surface Finish on the Friction and Wear of PCTFE Plastic on Mild Steel	1.0
2. On the Influence of the Degree of Crystallinity of PCTFE on its Transfer to Steel Surfaces of Different Roughnesses	2.0
3. Depth of Penetration as a Predictor of the Wear of Polymers on Hard, Rough Surfaces	3.0
4. Full Penetration Wear Model	4.0

LIST OF FIGURES

	Page
1. Pin-on-Disk Apparatus for Experiments in SEM	17
2. Wear Track Formed During Sliding in SEM	17
3. PCTFE Pin Prior to Sliding	18
4. PCTFE Pin After 10 Revolutions of Disk	18
Appendix 1	
1. Pin on Disk Machine	1.11
2. Mass Transfer of PCTFE to 1018 Steel for Various Surface Finishes and Number of Passes	1.11
3. Coefficient of Friction of PCTFE on 1018 Steel for Ground and Lapped Surfaces at Various Numbers of Passes During a 40 Pass Run	1.12
4. Coefficient of Friction for Surface Ground 0.68 μ AA 1018 Steel for First and Tenth Pass Showing the Influence of Sliding Direction-Lay Orientation	1.12
5. Initial Transfer of PCTFE to Steel Surfaces	1.13
6. Transfer of PCTFE to 0.7 μ AA Steel Surface	1.14
7. Transfer of PCTFE to Glass-bead Blasted Surfaces 1.2 μ AA	1.15
Appendix 2	
1. Pin-on-Disk Machine	2.19
2. Mass (a) and Mass Rate (b) Transfer as a Function of the Number of Repeated Passes of a PCTFE Pin on a 1018 Steel Surface Load 0.49N, Sliding Speed 0.935 cm/sec.	2.19
3. Mass Transfer as a Function of the Number of Repeated Passes of a PCTFE Pin on a 1018 Steel Surface, Load 0.49N, Sliding Speed 0.935 cm/sec.	2.20
4. Transfer of PCTFE to Radial and Circular Lay 1018 Steel Disks. Load 0.49N, Speed 0.935 cm/sec.	2.20
5. Transfer of PCTFE to Disk B. (a) Amorphous (b) Crystalline. Load 0.49N, Speed 0.935 cm/sec, 1000 passes.	2.21
6. Variations of Transfer of PCTFE to Steel as a Function of the Angle Between the Lay and the Sliding Direction	2.22

	Page
7. Autoradiograph of Transfer of PCTFE to Steel Disk, Load 1.96N, Speed 0.935 cm/sec., 200 passes	2.23
8. Transfer of PCTFE to Surfaces with Radial Lay, Load 0.49N, Speed 0.935 cm/sec.	2.24

Appendix 3

1. Scanning Electron Photomicrograph of Nylon 6/6 Transferred to a Rough Steel Surface; Full Penetration	3.3
2. Penetration Depth as a Function of Bearing Area for Several Disk, Polymer, and Load Combinations	3.5
3. Polymer Wear as a Function of Penetration Depth	3.5

Appendix 4

1. Force Diagram Showing Geometric Relationships Between Forces at Tool Point when no Built-Up Edge Exists [1].	4.3
2. Shearing Process on the Shear Plane [3].	4.5
3. Forces Acting on a Single Steel Asperity	4.9
4. S_s/p_m versus a for Different Values of k	4.13
5. Plot of ϕ versus k for Various Values of α	4.14
6. Volume of Material Removed by a Given Asperity for PVC and PCTFE	4.16

LIST OF TABLES

	Page
1. Tensile Test Results	11
2. Wear Rates of Doped LDPE, PVC, and PCTFE	13
Appendix 1	
1. Experimental Parameters, Conditions, and Variables	1.3
2. Coefficient of Friction of PCTFE Sliding on 1018 Steel for Various Surface Finishes and Number of Passes	1.5
3. Surface Profile Characterization	1.5
4. Initial Mass Transfer as a Function of Average Asperity Slopes	1.7
5. Correlation of Surface Parameters with Wear After 40 Passes	1.8
Appendix 2	
1. Surface Characterization of Disks	2.17
2. Interplanar Spacings of PCTFE as Extruded and Heat Treated	2.18
3. Mechanical Properties of PCTFE for Different Heat Treatments	2.17
Appendix 3	
1. Mechanical Property Data for Polymers	3.2
2. Experimental Variables	3.2
3. Shear Angle Measurements	3.3
4. Mass of Polymers Transferred to Circular Disks	3.3
5. Surface Statistical Parameters	3.4
6. Ratio of Real to Apparent Area of Contact	3.5
7. Wear and Profile Data	3.5
Appendix 4	
1. Wear Data for PVC and PCTFE Conical Polymer Pins Run on Steel Disks 11 and 22	4.16

1. INTRODUCTION

Polymers are known for their excellent combination of properties, rather than an extreme of any single property. For example, no polymer is as strong as steel, as light in solid form as most woods, as elastic as soft rubber, nor as scratch resistant or transparent as glass. Yet, polymers are the only materials which can be simultaneously strong, light, flexible and transparent [1]*. Typical polymer properties include high mechanical strength and rigidity, fatigue endurance, high resistance to moisture, excellent dimensional stability, ease of fabrication, resistance to repeated impacts, good electrical insulating characteristics, natural lubricity, noise and weight reduction and others. For these reasons, the polymer industry has seen a phenomenal growth over the past thirty-five years.

Polymers are used in a wide variety of engineering applications where high stresses are encountered. Some examples include drawer sliders, bearings in heart valves, gears, and artificial bone joints. Aside from the frictional behavior of a polymer, its wear resistance is most important in determining its acceptance in industry. Thus, it is important to be able to predict polymer wear, under many adverse conditions, and hence arrive at the life expectancy of a given component.

The performance of polymers in dry sliding contact is very difficult to predict. The wear resistance of the polymer is determined not only by its material properties, but also by external conditions such as load, speed and the roughness of the surface against which

*Numbers in brackets refer to similarly numbered references listed in Reference section.

relative sliding occurs. In the initial stages of the wear of a polymer against a harder counterface, polymer transfers to the counterface. If the counterface is smooth, some polymers such as polytetrafluoroethylene (PTFE) and high density polyethylene (HDPE) transfer as continuous thin films via the adhesion mechanism [2]. If the counterface is rough, most polymers will transfer in discrete lumps via the abrasion mechanism [3-5]. As sliding continues other mechanisms such as fatigue may dominate the transfer process [4-5]. In addition to transfer to the counterface some polymers wear by roll formation [5]. The initial transfer process is often complicated by back transfer in which two or more wear mechanisms can be equally important.

For some of the above mechanisms, such as the thin film transfer to smooth surfaces, no quantitative models have been developed even though the transfer process has been demonstrated to depend on a very smooth, harder counterface and a polymer having a smooth molecular profile [2]. For other mechanisms, such as abrasive wear, quantitative models have been postulated. One model for abrasive wear predicts that abrasive wear is proportional to normal load, sliding distance, the average slope of the asperities of the harder counterface, and inversely proportional to the flow pressure of the polymer [6]. However, experiments [3] do not confirm the predicted proportionality with average asperity slope. Another model predicts that abrasive wear is proportional to the coefficient of friction μ and the normal load p and inversely proportional to the polymer hardness H , strength σ , and elongation e at fracture [7]. Experiments of several polymers abraded on emery paper resulted in a linear positive correlation between $\log \mu/H\sigma e$ and

abrasive resistance.

None of the proposed models can predict abrasive wear for a given polymer on a given surface, even though the models may successfully predict the relative rankings of different polymers rubbing on the same surface or the same polymer rubbing on different surfaces. Hence, most of the experiments on wear reported in the literature have measured wear coefficients (constants of proportionality) for one wear model. Some researchers [8] believe that wear models must be based on polymer properties which are measured under conditions of stress, strain rates, and temperature which are representative of the conditions existing in sliding. The crucial questions are: which properties should be measured and what should be the conditions of measurement?

In addition to the measurement of material properties, measurement and characterization of the surface topography on which the polymer slides are necessary inputs to wear models for polymers. The researcher is confronted with the problems of deciding which instrument to use to measure the surface, how much of the surface to measure, and which parameters should be used to characterize the surface. For example, Rabinowicz's [6] abrasive wear model includes the average slope of the surface profile as the parameter to characterize the surface whereas Ratner's [7] wear model has no surface parameter. Obviously, Ratner's model is only useful for ranking the abrasive wear resistance of polymers on a given surface. However, as noted above abrasive wear did not correlate with the average slope of asperities in experiments of cones ploughing grooves on polymers.

Clearly, models for the wear of polymers must include both polymer

properties measured under conditions found in sliding and surface topography parameters. Thus, it was the objective of the research reported here to determine the material properties and the parameters of surface topography characterization which are significant in the wear of polymers. A quantitative measure of the initial stages of wear was made possible by using neutron activation analysis to measure the polymer transferred to counterfaces. Identification of the significant polymer properties and surface features was made possible by direct observation of the wear process, transferred polymer, and wear scars on polymer sliders in the scanning electron microscope.

Polymer wear models were postulated for the initial stages of sliding for two combinations of load-pin geometry: one in which the apparent and real areas of contact were approximately equal (full penetration) and one in which the apparent area was much larger than the real area (partial penetration). The models included polymer properties and surface characterization parameters.

2. SUMMARY

2.1 Wear Measurement by Neutron Activation Analysis (NAA)

A wear measuring technique using radioactive tracers was developed which was capable of detecting less than one microgram of polymer transferred to a counterface. The technique requires that the polymer contain an element which can be activated by neutron bombardment with exposure times short enough not to cause significant polymer property changes. The half life of the activated elements must be long enough to permit wear experiments to be run and to count the activity of the

transferred material before the activity decays to background levels. Polymers containing chlorine such as polychlorotrifluoroethylene (PCTFE) and polyvinylchloride (PVC) are suitable. Other polymers may be doped with small quantities (one percent) of suitable elements, such as dysprosium, and successfully measured by this technique. Experiments have shown that the mechanical properties of low density polyethylene (LDPE) are not significantly affected by the doping agent. The technique also has potential use for filled polymers, in which elements in the fillers are activated and traced.

The major advantages of the technique are the capability of detecting less than a microgram of transferred polymer, an insensitivity to the effects of environment, especially moisture and dust, on the wear measurement, and the capability of measuring dynamic wear phenomena such as back transfer. The disadvantages of the technique are the requirement for a NAA laboratory, handling of radioactive materials, and some limitations in the polymers which may be activated as noted above.

2.2 Observations in the Scanning Electron Microscope (SEM)

Observations of the transferred polymer, wear scars on the polymer sliders, and dynamics of the wear process provided valuable insight required for the correct choice of parameters to include in wear models. Lump transfer was observed on all steel surfaces (hand lapped, ground, and bead blasted) for PCTFE, PVC, Nylon 6/6, and LDPE. The location of the transferred material was highly correlated with the topographical features of the surface. On hand lapped surfaces, the polymer transferred

in the scratches on the surface which were caused by the lapping abrasive particles or by the prior grinding operation. On ground and bead blasted surfaces, the polymer initially transferred at the highest peaks and ridges. Subsequently transferred material gradually filled the valleys between the highest peaks. Polymers fully penetrated by the steel asperities initially transferred by shearing off at the highest asperities. The transferred polymer filled in the slopes of the asperities, shearing along a plane which made an acute angle with the horizontal. The shear angle was significantly different for PCTFE, PVC, and Nylon 6/6 being 12.4, 10.9, and 19.0 degrees, respectively.

The quantity of polymer transferred was found to be dependent on the relation between the sliding direction and the lay of the surface. The amount of transfer was least where sliding parallel to the lay, intermediate when sliding perpendicular to the lay, and highest when sliding at an acute angle to the lay. For multiple passes over the same track, sliding parallel to and perpendicular to the lay resulted in the polymer filling the valleys between the highest ridges. When the valleys were filled, the wear rate decreased almost to zero. On the other hand, when sliding at an angle to the lay, the polymer deposited in the valleys was moved along the valley by the friction forces until it piled up at the edge of the wear track. Hence, the wear rate remained at a finite, non zero value.

A wear experiment was designed which could be performed in the SEM. Observations of the dynamics of the wear process confirmed the build-up of polymer deposits at the high points on the counterface. The experiments also showed that prows of polymer were formed at the

trailing edge of the wear scar from material extruded from the interface and back transferred from deposits on the counterface. These prows would build-up and then break off falling on the track. Subsequent passes would either push these fragments to the side of the track or else ride over the fragments embedding them into the polymer wear scar. The energy dispersive x-ray attachment to the SEM was indispensable in distinguishing deposited polymer from artifacts and contaminants.

2.3 Wear Model Development

During the reported research, the wear of polymers was found to have a positive correlation with a variety of polymer properties and surface topography parameters. For example, wear of PCTFE heated treated to obtain different elongations at break, was shown to correlate positively with the inverse of the energy-to-rupture of the polymer. Wear of PCTFE was found to correlate with the average asperity slopes for initial passes over a rough steel surface and with the product of the arithmetic average roughness and correlation length for repeated passes over the surface. However, as experiments continued it became clear that a wear model must include both the polymer properties and the surface topography parameters which are important to the wear process.

An important finding was that surfaces machined to the same arithmetic average roughness by the same machine and operator almost always had differences which had significant influence on the wear process. For example, in lightly loaded systems, it was the uppermost portion of the profile which caused the polymer wear. Hence, surfaces with similar arithmetic average roughnesses based on the entire

surface profile sampled, had greatly different distributions of asperity heights in the upper five to ten percent of the profile. These differences were dramatically revealed by the bearing areas curves for the profile. The best correlations of wear with surface parameters and polymer properties were obtained when wear was correlated with the penetration depth, and the shear angle of the polymers. The shear angle of the polymers was related to orthogonal cutting theory. The theory predicted the asperity slopes necessary to cause the polymer to shear and the shear angle. However the angles predicted were much larger than measured indicating that more accurate data on polymer mechanical properties, such as shear strength in sliding contact are needed.

3. DISCUSSION

3.1 Wear Measurement by Neutron Activation Analysis (NAA)

One of the objectives of this research was to study the transfer of polymers to hard counterfaces. Because polymers have been demonstrated to transfer in very thin films on smooth surfaces it was anticipated that a sensitive wear measuring technique was required. Gravimetric and volumetric wear measurements neither had the sensitivity nor the precision needed. Therefore, a radiotracer technique was developed using neutron activated isotopes in the polymer as tracers. The technique is completely described in [9] which is readily available internationally and reprints have been previously delivered to U.S.A.R.O. for limited distribution. Since this reference has been published, the technique has been modified and extended to include a wider range of polymers.

Two techniques have been used to detect the quantity of radioactive isotopes. The first technique [9] consisted of detecting all gamma radiation from the activated polymer in an energy bandwidth with included the two major energy peaks from ^{38}Cl , 1.60 and 2.15 MeV. The second technique, Appendix 2, consisted of measuring the energy in each major peak individually. For those isotopes, such as ^{38}Cl which had more than one major peak the mass transferred was determined for each peak and then an average was reported. The computer algorithm for determining the area under the energy peaks is given in [10].

While it is possible to determine the mass of isotopes present by using internal calibrations in the NAA program, these calibrations are based on the sample being at the geometric center of the detecting crystal. Because wear tracks are circular with radii from 1 to 1.5 cm, the tracks are not located over the center of the detector during counting. Hence, direct calibrations were made by weighting samples of polymer, irradiating and then placing the samples at various distances from the center of the detector. The effect of radius on radiation detected is given in [9].

Because only two engineering polymers contain chlorine, PCTFE and PVC, a doping technique was investigated to extend the applicability of the radiotracer technique to other important engineering polymers. One percent by weight of powdered Dy_2O_3 was mixed with powdered low density polyethylene (LDPE), then injection molded. Tensile specimens and wear pins were machined from the molded material. Undoped LDPE was processed and machined under the same conditions as the doped LDPE for comparison of mechanical properties and wear.

Two qualitative observations were made on the effect of processing and straining on the crystallinity of the LDPE. The first observation was that the injection molding caused the doped LDPE to be more opaque and whiter than the undoped LDPE. This result was expected because the Dy_2O_3 has the properties necessary to be a nucleating agent for polymer crystals. These properties include a higher melting point than the polymer, insolubility in the polymer melt, and no chemical reactivity with the polymer [11].

The second observation was that during tensile testing the necking process caused the undoped polymer to whiten and become more opaque whereas no discernible changes were noted in the doped polymer. As noted in Table 1 there were no significant differences between the elongation at rupture for the doped and undoped polymers. Hence, the straining during necking has caused an increase in crystallinity of the undoped LDPE to the level found in the doped polymers after injection molding.

The other tensile properties measured in the tensile tests are given in Table 1. Only the tensile strength at yield was found to be significantly different for the two polymers, the difference being only 3.5 percent. The elongation at break, a property which Ratner [7] has determined as being important in the abrasive wear of polymers, was almost identical for the doped and undoped polymers.

No quantitative wear data was obtained on the undoped LDPE, thus no direct comparison of the wear of the doped and undoped LDPE could be made. However, pins made from each were worn under identical conditions (normal load, 0.49N, sliding speed 0.935 cm/sec, track

TABLE 1. Tensile Test Results

<u>PROPERTY</u>	<u>DOPED</u>			<u>UNDOPED</u>		
	<u>Number of Samples</u>	<u>Value</u>	<u>Standard Deviation</u>	<u>Number of Samples</u>	<u>Value</u>	<u>Standard Deviation</u>
Tensile Strength at yield, MN/m ²	11	8.63	0.07	11	8.94	0.16
0.2% Offset Yield Strength, MN/m ²	9	5.70	0.24	12	5.76	0.63
Energy-to-Rupture, MNm/m ³	9	9.65	1.97	9	8.32	1.06
Elastic Modulus, MN/m ²	9	288.18	61.42	11	322.21	66.48
Elongation to Break, %	9	102.72	10.31	6	102.14	12.87

circumference 9.5 cm, 750 revolutions of the disk) and the wear tracks were examined in the scanning electron microscope. There was no significant difference between the appearances of the two wear tracks.

Quantitative data was obtained on the wear of the doped LDPE which was compared to the wear of PVC and PCTFE on the same surface. These results are given in Table 2. Discussion of these data in relation to wear models is included in Appendix 4. The sensitivity of the NAA technique for wear measurement can be extracted from the data by noting that sliding distances were 0.5 m. Hence, a wear rate of $0.17 (10)^{-9}$ kg/m was calculated from 0.09 μ gm of polymer on the disk. The standard deviation for this small quantity of polymer transferred is 29% of the amount transferred. This standard deviation is determined by the decay statistics of the isotope and the background count in the laboratory. It is not a result of repeated experimental runs. Hence, a standard deviation can be reported for only one run which gives one data point.

3.2 Scanning Electron Microscope Observations

On the surfaces prepared for the wear experiments the predominant mode of transfer was lumpy transfer. The transfer was almost always associated with the prominent surface features as shown in Fig. 5-7, Appendix 1. If thin film transfer did occur it was present in quantities which could not be observed in the SEM or detected by the energy dispersive x-ray analysis of the wear tracks. Transfer occurred on the first pass over the surface at widely scattered sites. As repeated traversals were made over the same wear track the number of sites where polymer transferred increased and the quantity of polymer at each site

TABLE 2. Wear Rates of Doped LDPE, PVC, and PCTFE

Disk Roughness $R_a, \mu m$	Wear Rate (Kg/m) ***		
	LDPE	PVC	PCTFE
0.10*	0.929×10^{-9} (.063)**	0.22×10^{-9} (0.05)	0.17×10^{-9} (0.05)
0.34	8.599 (0.155)	20.10 (0.67)	7.69 (0.34)

*Radial lay, arithmetic average roughness, R_a , measured perpendicular to lay.

**Standard deviation

***Spiral track, normalized by sliding distance, normal load 1.96N, sliding speed 0.935 cm/sec average

also increased as shown in Fig. 6, Appendix 1.

Usually the surfaces observed in the SEM were at an angle to the electron beam between 90 and 60 degrees. Using a special fixture, some surfaces could be located at angles of 0 to 30 degrees to the electron beam. In these latter positions details of the transfer process were revealed that could not be observed in the former orientations. In Fig. 1, Appendix 3, it is noted that the polymer sheared off at an angle to the horizontal. Over 200 photographs of these polymer deposits were taken and over 700 angle measurements were made of the shear angles for three polymers, PVC, PCTFE, and Nylon 6/6 and three normal loads, 2.45, 9.80, and 14.7 N. The results are summarized in Table 3 in Appendix 3. These observations of the shear angle formed an important input into the development of a wear model for the polymer transfer process.

The quantity of polymer deposited is a function of the sliding direction with respect to the lay of the surface. This was revealed when the wear track on the disk surface which had been unidirectionally ground was observed as shown in Fig. 6, Appendix 2. The dark deposits are the polymer (PCTFE) transferred to the surface during repeated passes over the same track. Several features of this wear track are significant. The wear track is darkest when the sliding velocity vector is at an angle of 10 to 80 degrees to the lay direction, indicating that the greatest amount of polymer is in this portion of the wear track. In addition, a row of debris appears at the edge of the wear track. The debris shows up as white particles because they are bulkier than the polymer deposits in the wear track and they are less intimately in

contact with the conducting steel surface of the disk. Hence an electron charge on the particles caused them to appear bright. It should be noted that as the sliding vector passes through the lay direction the debris shifts from the inside to the outside of the wear track.

The presence of these arcs of loose debris particles at the edge of the wear track suggest a mechanism of transfer. The highest asperities on the steel surface remove polymer which is deposited on the valleys. Continued sliding over the same track results in more polymer being deposited in the valleys. In addition, there is some friction between the deposited polymer and the polymer slider. The component of the friction force parallel to the lay, moves the deposited polymer to the edge of the track. Hence, the debris appears on the inside of the track when the component of the friction force parallel to the lay points to the inside of the circle.

When the sliding vector is parallel to the lay the amount of polymer deposited is least. These observations have been confirmed by autoradiographs of the wear track on a unidirectionally ground surface as shown in Fig. 7, Appendix 2. The autoradiograph qualitatively confirmed wear data in Appendix 2 which indicated that wear rates were highest when the sliding vector was at an angle to the lay, intermediate when perpendicular to the lay and least when parallel to the lay.

The implications of these observations on wear model development are important because they indicate that wear rates measured on an anisotropic surface topography will vary by an order of magnitude or more as a function of the angle that the direction of the sliding vector

makes with the direction of lay. Hence, specifying a roughness parameter such as arithmetic average is insufficient information for quantitative wear prediction.

Direct observations of the wear process were obtained on a small pin-on-disk machine which was mounted in the SEM, Fig. 1, 2. The normal load was supplied by a cantilever spring. The disk was rotated by a mechanical linkage which could be turned by hand or driven by a constant speed motor from outside the specimen chamber of the SEM. It was possible to locate specific surface features in the wear track and examine those areas after successive passes of the pin over the same spot.

Observations of the pin-disk contact area during sliding showed the build-up and subsequent break off of prows of polymer on the trailing edge of the pin, Fig. 3, 4. It is postulated that these prows consisted of polymer plastically flowed out of the interface as well as polymer pulled out of the track as the trailing edge of the polymer pin passed over the transferred polymer. Prows which broke off were either pushed to the side of the track or else picked up again by the pin on a subsequent pass.

By observing polymer deposited at a site on the steel disk on successive passes, the deposits were observed to grow and decrease in size. The decreases occurred when the pin picked up deposited polymer from the disk. These observations of the dynamics of the transfer--back transfer process emphasize the random nature of the transfer process. In fact, it is surprising that there is not more scatter in the wear data than that which has been measured.

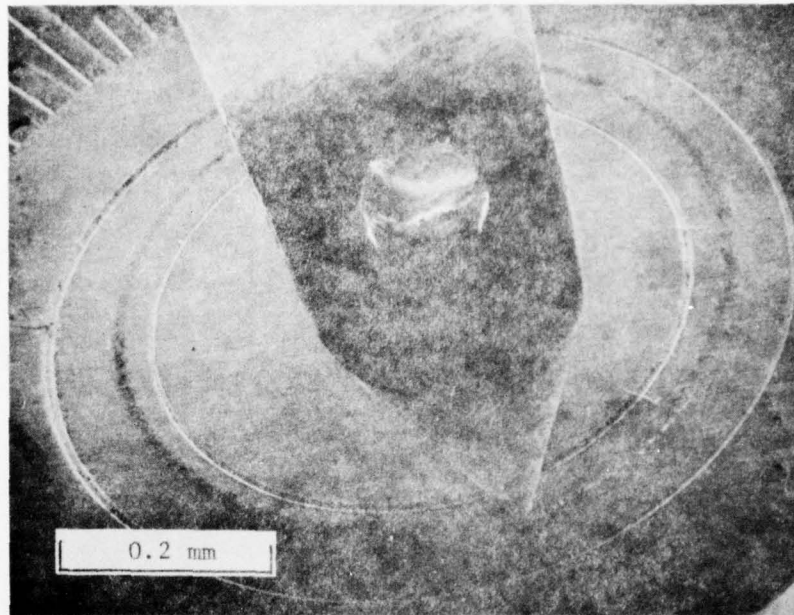


Figure 1 Pin-on-Disk Apparatus for Experiments in SEM

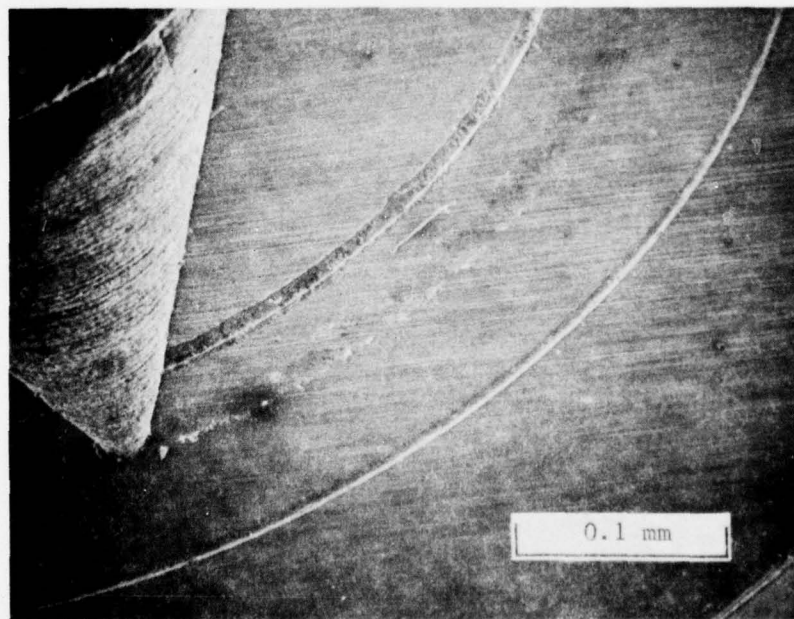


Figure 2 Wear Track Formed During Sliding in SEM

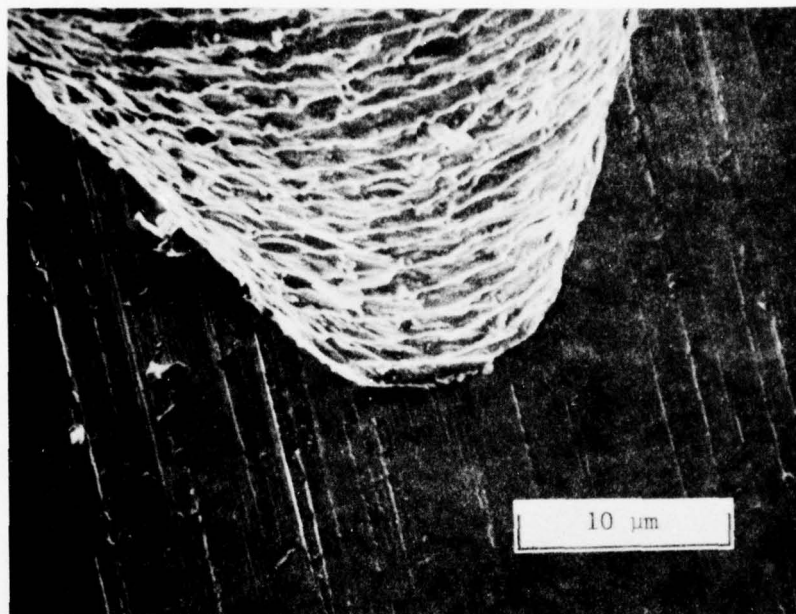


Figure 3 PCTFE Pin Prior to Sliding

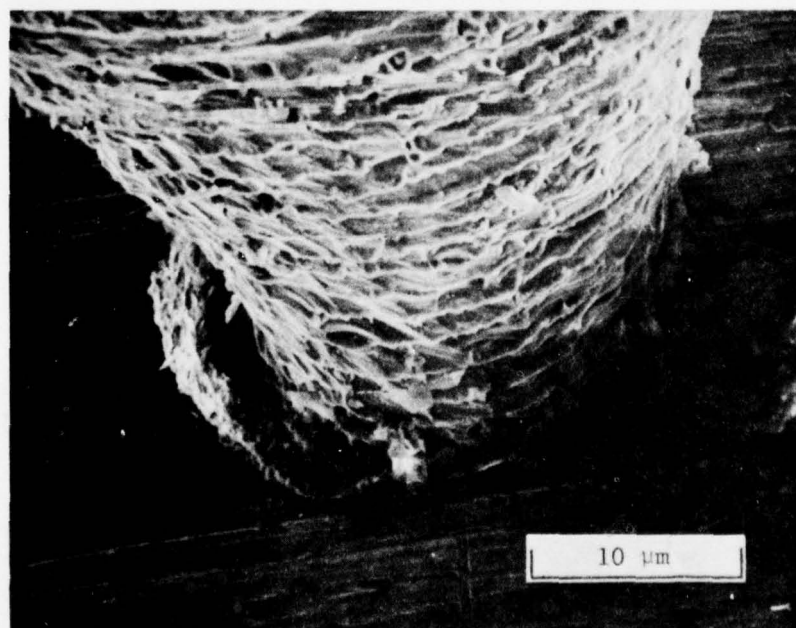


Figure 4 PCTFE Pin After 10 Revolutions of Disk

3.3 Wear Model Development

The development of a wear model for the transfer of polymers to harder rough surfaces has proceeded as follows: development of a sensitive wear measuring technique which has been used to test various wear models postulated, microscopic observations of the wear process by the SEM which have been used to identify factors important in the transfer wear process, formulation of wear models using the factors found to be important, and testing the range of validity of the wear models. The experience obtained in this research has confirmed that better wear models will be formulated from the results of more careful and more sensitive observations of the wear process. The picture of the abrasive wear process which is emerging for polymers is dominated by the importance of the surface topography of the counterface and the deformation and resistance of the polymer to penetration.

In the early experiments on this program the wear of PCTFE was positively correlated with the average asperity slope of the steel surfaces on which it was slid, Table 4, Appendix 1. This correlation on the initial pass over the surface was not linear as the simple abrasive wear theory predicts. For several passes over the surface the polymer begins to fill up the valleys on the surface. The wear was found to correlate with the arithmetic average roughness, a measure of the profile heights, times the auto correlation length, a measure of the spacing between profile peaks, Table 5, Appendix 1. This product was chosen to represent the volume of space available between peaks for polymer to deposit on the surface. This work indicated that there can be two or more parameters which will correlate with wear (e.g.,

arithmetic average roughness, and average asperity slope). However, without a physical basis for relating wear to the parameter, its correlation with wear may be fortuitous and of limited validity.

Thus, one thrust of the research was to obtain as extensive a characterization of the counterface surfaces as possible. The surfaces were characterized by measuring the topography by line profiles obtained from a stylus moved over the surface. The profile was then digitized and used to calculate a wide variety of surface topography parameters (Table 5, Appendix 3 and Ref. 12). Parameters were calculated from the entire profile data (arithmetic average roughness and auto-correlation function, for example) and from truncations of the profile data (average slope of the upper 5 percent of the profile). The need for calculation of parameters based on the complete and partial profile data was recognized when calculations revealed that some load-geometry combinations resulted in complete penetration of the asperities into the polymer while other combinations resulted in only partial penetration.

It became clear that abrasive wear depended on the interrelation between normal load, surface topography, slider geometry, sliding direction with respect to lay, repeated traversals over the same track, and polymer mechanical properties. Therefore, the wear process was broken down into stages and effort was started to develop models for each stage. These stages of wear described in the following paragraphs are based on the observations of wear tracks, wear scars, and wear debris in the SEM and on wear measurements.

When a polymer pin was loaded against a steel surface, the polymer was deformed by the penetrating steel asperities until sufficient real

area of contact developed to support the normal load. If the initial geometry of the pin was conic, then it was assumed that the real and apparent areas of contact were approximately equal. This condition was called full penetration. If the initial geometry of the pin was a truncated cone, then the real area of contact was less than the apparent area of contact. This condition was called partial penetration.

When sliding started (by moving the steel surface relative to the pin) polymer transferred to the steel surface. For full penetration, the polymer sheared off at an angle (as shown in Fig. 1, Appendix 3), the angles being significant for different polymers, Table 3, Appendix 3. The steel surface which passed under the pin was not completely covered with polymer deposits. Thus, some topographic features of the surface did not have the correct geometry to cause the polymer to shear and fracture during sliding.

For partial penetration, when sliding was initiated, the process of polymer transfer is similar to material removed by chip forming processes. The polymer in the path of an asperity sheared along a shear plane and began to fill up the volume between the steel surface and the surface of the polymer pin not in contact at the asperities. However, polymer transfer differs from chip forming models in that chip forming models assumed that all material in the path of the tool is removed, whereas, for certain geometry asperities, the polymer can flow around the asperity without being removed as a chip or loose wear particle.

For repeated traversals over the same path and full penetration, the wear rate dropped off rapidly on subsequent passes as the polymer pin was sliding on transferred polymer and little additional removal

occurred. However, if the surface had a lay and the sliding direction was at an angle to the lay, polymer continued to transfer by the mechanism described in Section 3.2. For partial penetration, the wear continued until the space between the bottom of the polymer pin and the surfaces became filled with transferred polymer. Then, the wear rate began to diminish.

A model for full penetration wear, based on orthogonal chip forming theory and the polymer shear angle measurements is described in Appendix 4. The model was of limited success in that it predicted the relative rankings of the wear of two polymers. However, the shear angles predicted by the theory were much higher than actually measured. The difficulty was ascribed to inadequate knowledge of the polymer properties which must be used in the shear angle calculations. This difficulty in defining the polymer properties to use in wear models must eventually be solved by using properties measured in the stress and strain conditions existing in sliding systems.

A model for partial penetration wear, based on depth of penetration of the steel asperities into the polymer and the measured polymer shear angles, was successful in predicting the relative wear of two polymers. However, depth of penetration, being based on the extreme heights of the profile and on polymer flow pressure, is subject to error from unrepresentative sampling of the surface-profile and from the incorrect polymer flow pressure used to determine the real area of contact.

While the wear models developed at the end of this research show promise for predicting polymer wear and transfer, a continuing experimental and theoretical program is required to increase the

confidence in the predictions from these models. It is clear that complete surface characterization is required as is the measurement of polymer properties under conditions which exist in sliding systems.

4. References

1. Dourlet, E. F., "Selecting Plastics," Machine Design, Plastics/Elastomers Reference Issue, 1971, pp. 1-4.
2. Briscoe, B. J., C. M. Pooley, and D. Tabor, "Friction and Transfer of Some Polymers in Unlubricated Sliding," Advances in Polymer Friction and Wear, L. H. Lee, Ed., Volume 5A, Plenum Press, New York, 1974, p. 191.
3. Lancaster, J. K. "Abrasive Wear of Polymers," Wear, 14, 1969, p. 223.
4. Lancaster, J. K., "Basic Mechanisms of Friction and Wear of Polymers," Plastics and Polymers, 41, 1973, p. 297.
5. Lee, L. H., "Effect of Surface Energetics on Polymer Friction and Wear," Advances in Polymer Friction and Wear, L. H. Lee, Ed., Volume 5A, Plenum Press, New York, 1974, p. 31.
6. Rabinowicz, E., Friction and Wear of Materials, John Wiley and Sons, New York, 1965.
7. Ratner, S. B., I. I. Farberova, O. V. Radyukevich, E. G. Lur'e, "Connection Between Wear Resistance of Plastics and Other Mechanical Properties," Soviet Plastics, 1964, (Plast. Massy, 1963), No. 7, 37, pp. 145-160.
8. Briscoe, B. J., private communication.
9. Eiss, N. S., Jr., S. D. Doolittle and J. H. Warren, "An Application of Neutron Activation Analysis to the Measurement of the Wear

of Polymers, Wear, 38, No. 4, 1976, pp. 127-143.

10. Roscoe, Bradley A., and A. K. Fien, "Algorithm for Computer Processing and Analysis of Gamma Ray Spectra for Large Scale Laboratory Operations", Nuclear Instruments and Methods, 137, May 1976, pp. 173-178.
11. Chatterjee, A. M., "Heterogeneous Nucleation in the Crystallization of High Polymers from the Melt," Ph.D. Dissertation, University of Massachusetts, 1974.
12. Eiss, N. S., Jr., and J. H. Warren, "Current Advances in Surface Characterization," ASME Paper No. 76-DET-88.

APPENDIX 1

The Effect of Surface Finish on the Friction
and Wear of PCTFE Plastic on Mild Steel

by

Norman S. Eiss, Jr.
Associate Professor

Jeffery H. Warren
Research Assistant

Mechanical Engineering Department
Virginia Polytechnic Institute and State University
Blacksburg, Virginia 24061

Society of Manufacturing Engineers

Paper No. IQ75-125

Revised 25 April 1975

The Effect of Surface Finish on the Friction and Wear of PCTFE Plastic on Mild Steel

by

Norman S. Eiss, Jr., Associate Professor
and

Jeffery H. Warren, Research Assistant

Mechanical Engineering Department
Virginia Polytechnic Institute and State University
Blacksburg, Virginia 24061

ABSTRACT

An experimental study of the friction and wear of polychlorotrifluoroethylene (PCTFE) rubbing on mild steel was performed on a pin-on-disk machine, with a normal load of one kilogram and a sliding speed of 0.2 cm/sec. Four different surface finishes were used, glass-bead blasted, 1.26 μm AA; surface ground, 0.7 and 0.14 μm AA; and lapped, 0.07 μm AA. The friction and wear on initial passes were found to correlate with AA roughness and average asperity slope. On repeated passes, the friction and wear were mostly influenced by the properties of the transferred polymer-polymer interface. After 40 passes, the wear was found to correlate with the product of the AA roughness and the correlation length. It was concluded that parameters calculated from only the upper portions of the profile have the most promise for correlating with friction and wear phenomena occurring at the highest asperities, rather than parameters based on the entire profile.

INTRODUCTION

The increasing use of plastics as replacements for metals in applications where sliding contact occurs between two machine elements is due to several advantages that plastics have over metals. Plastics have good combinations of properties rather than extremes of any single property. For example, nylon and PTFE are outstanding dry bearing materials not merely because of their low coefficients of friction but also because they offer a combination of good abrasion resistance and corrosion resistance, fair-to-good creep resistance and an ability to engulf abrasive particles. Another important advantage of plastics is that parts can be produced with fewer fabricating operations. Parts require a minimum of finishing after processing because color, surface texture, threads, undercuts and metal inserts can all be obtained during the molding process.

The applications of plastics has far outrun the basic understanding of the mechanisms of phenomena such as friction and wear. This lack of understanding prevents designers from predicting wear and friction in a given application unless test data is available from a similar application. Lacking test data, the designer is forced to run screening tests of materials for those applications where friction and wear properties are critical for proper performance. Thus, a need clearly exists for basic understanding of friction and wear of plastics.

The status of our understanding of friction and wear of plastics has been summarized by Steijn [1] and Lancaster [2]. When studying wear phenomena, the initial surface finish is usually of little interest because the wear process is continuously modifying the surface. However, when a plastic slides on a metal surface, the metal surface suffers relatively little change as the plastic is worn away and transfers to the metal surface. The limited data found in the literature on the effect of surface finish on plastic wear [2] show that wear has a positive correlation with AA roughness. Other studies [3] have shown that the curvature of the surface has a positive correlation with wear of plastics.

An increasing number of investigators are recognizing that several parameters can be used to characterize a surface [4]. It was the purpose of this work to investigate the relation between surface characterization parameters and friction and wear of a plastic, PCTFE, sliding on mild steel.

EXPERIMENTS

Purpose

The purpose of the experimental program was to measure the wear and friction force of a plastic rubbing on a harder metal surface. The major independent variables were the AA roughness of the metal surfaces and the method of producing the surfaces. All other parameters, such as normal load, sliding speed, materials, environmental conditions, and geometry of the experimental materials were fixed.

Apparatus

A pin-on-disk machine, shown in Figure 1, was used to provide the relative motion between the materials. The plastic pin, A, 3.175 mm diameter and 3.175 mm long was mounted with its axis parallel to the surface of disk, B, and parallel to the relative sliding velocity vector. The pin was attached to an arm, C, which pivoted vertically at D and horizontally at E. Horizontal motion of the beam was restrained by a cantilever beam, F, on which were mounted strain gages, G. The output of the strain gages was plotted on an X-Y recorder and calibrated to read friction coefficient. The normal load was applied by dead weight, H. The disk rotation was controlled by a variable speed transmission and the power was supplied by a 1/2 HP synchronous motor. The radius of the path of the pin on the disk was controlled by moving the pivot support, I, in the directions indicated.

Experimental Variables, Parameters, and Conditions

The parameters, conditions, and variables for the experiments are given in Table 1.

* Numbers in brackets refer to similarly numbered references listed at the end of the paper.

Table 1

Experimental Parameters, Conditions, and Variables

<u>Parameter</u>	<u>Pin</u>	<u>Disk</u>
material	PCTFE *	1018 cold rolled steel
diameter	3.175 mm	76.2 mm
thickness	3.175 mm	6.35 mm
contacting surface	as extruded	glass-bead blasted, surface ground, hand lapped.

* polychlorotrifluoroethylene

Operating Conditions

Normal load: 1 kg

Sliding speed: 0.2 cm/sec.

Atmosphere: Air at 73° F, 50-60% Relative Humidity

Lubrication: None

Variables

<u>Surface preparation of disk</u>	<u>AA (μm)</u>
Surface grind to 0.8 μm AA, then Blast with glass beads .074 to .147 mm dia	1.26
Surface grind, unidirectional with Aluminum oxide, 46 grit	0.68 0.135
Surface grind to 0.12 μm AA, Hand lap, 400 grit SiC, dry, unidirectional	0.067

Materials Preparation

The disks were finished as indicated in Table 1 and stored in light oil to prevent rusting. Just prior to running an experiment the disks were rinsed with methanol and put on the machine. The pins were cut to size from 3.175 mm dia. extruded rod, rinsed in pentane, air dried and sealed in polyethylene vials.

Wear Measurement

Because of the small amounts of material transferred in the initial phases of wear, a wear method had to be used which was accurate and sensitive. A radio-tracer technique which is described in detail elsewhere [5] was selected. The technique requires that the element

to be traced can be activated in the neutron flux of a reactor and that the activated element have a half life long enough to permit running an experiment and counting of the activity of the transferred material subsequent to the experiment. Of those elements found in commonly used plastics, only chlorine has the desired characteristics, its half life being 37 minutes. Therefore, PCTFE was selected as the experimental material.

In a typical experimental run the polyethylene vial with the PCTFE pin inside was inserted in the reactor for 10 minutes. After irradiation the vial was opened and the pin mounted in the arm (C, Figure 1). The normal load was applied and the disk was rotated for a predetermined number of revolutions. Friction measurements were made periodically during the run. At the conclusion of the run the disk was removed and taken to the radiation counter where it was counted for 30 minutes. The mass transferred was determined from a calibration curve of total counts as a function of mass.

To determine the relationship between the amount of PCTFE transferred and the number of repeated passes over the same surface a separate run was made for each of several predetermined numbers of passes. Each run was made on a different radius path on the same disk.

RESULTS

The PCTFE transferred to the steel disk as a function of the number of passes and the AA surface finish is shown graphically in Figure 2. Because each experiment for each number of passes on a given surface was run at a different radius, the sliding distance for one revolution was different for each run. The polymer transferred was normalized to an equivalent sliding distance at a radius of 11.2 mm by multiplying each value of mass transferred by the ratio 11.2 mm to the radius of the track. All data points represent the mean of three separate measurements, each on a different disk, except for the data at 120 passes (one measurement), the data for the hand lapped surface (one measurement at 10 and 20 passes and two measurements at one and 40 passes), and the data for the bead-blasted surface at 40 passes (two measurements).

The coefficient of friction data is summarized in Table 2. The coefficient of friction was monitored during each run. Thus, a time history of the friction force could be obtained for each single mass transfer measurement. It was found that during each run the coefficient of friction remained nearly constant when the two rougher surfaces were being rubbed. However, when the two smoother surfaces were rubbed a gradual increase in the coefficient of friction was observed as a function of the number of passes, as is shown in Figure 3.

On the surfaces which had a "lay" (all except the glass-bead blasted surfaces) a significant change in the coefficient of friction was occasionally noted when the sliding direction changed from parallel to perpendicular to the lay. The difference was most pronounced on the first pass of a run and decreased as the number of passes increased as shown in Figure 4.

Table 2

Coefficient of Friction of PCTFE Sliding on 1018 Steel
for Various Surface Finishes and Number of Passes

SURFACE/AA	Number of Passes					
	1	5	10	20	40	120
Bead-blasted/1.26 μm	.34**	.25	.28	.24	.28*	---
Surface ground/0.68 μm	.29**	.22**	.26	.28	.31	.24*
Surface ground/0.135 μm	.18	.20	----	.28	.26	.16*
Hand lapped/0.067 μm	.14**	.18*	.24*	---	.18**	---

All coefficients of friction are the mean of three measurements, each averaged over the last pass of each run, except those footnoted as follows:

* One measurement

** Mean of two measurements

One sample of each type of surface was characterized by taking a stylus surface profile and computing several statistical parameters. The results are given in Table 3 below.

Table 3

Surface Profile Characterization

Method of Preparation	AA μm	Average Slope	Average** Wavelength (μm)	Correlation Length*** L(μm)	AAxL μm^2
Glass Bead Blasted	1.26	.135	58.7	34.2	43.1
Rough Surface 90°*	0.68	.170	25.2	17.1	11.7
Ground 0°	0.30	.037	50.9	47.5	14.2
Smooth Surface 90°	0.135	.039	21.7	15.2	2.9
Ground 0°	0.078	.007	70.0	142.5	11.1
Hand Lapped 90°	0.067	.0226	18.6	15.2	1.0
0°	0.075	.0131	36.0	26.6	2.0

*Direction of stylus travel with respect to lay.

**Average Wavelength = $\frac{2\pi(\text{AA})}{\text{Average Slope}}$ [4]

***Distance profile must be shifted for the autocorrelation function to drop to 10 percent of its zero shift value

DISCUSSION

Lancaster [2] has identified three major types of wear of polymers: abrasive wear, fatigue wear, and adhesive wear. Abrasive wear is caused by hard asperities on the metal surface penetrating the polymer and ploughing and abrading the polymer surface. Fatigue wear is the detachment of material as a result of cyclic stress variations on a localized scale. Adhesive wear is the transfer of material from one surface to another as a consequence of the forces of adhesion between them.

For the initial pass over the metal surface, the abrasive wear of the polymer will predominate. The data in Figure 2 shows that the wear on the first pass is approximately proportional to the AA roughness of the surfaces. However, fortuitous as this correlation may appear, it is impossible to relate the single parameter of AA roughness to the mechanism of abrasive wear. The AA roughness contains no information on the spacing of the asperities in the metal profile nor on the shapes of the asperities.

The simplest theory on abrasive wear assumes that asperities of a hard surface penetrate a softer material and remove material by cutting or shearing [6]. The model leads to the relationship

$$v = \frac{Kw\ell \tan \theta}{p}$$

where v is the volume removed per asperity, w is the normal load per asperity, ℓ is the sliding distance, p is the flow pressure of the softer material (approximately equal to indentation hardness), θ is the angle of slope of the asperity, and K is a constant to account for the geometry of the asperity and the probability of some ploughing of the softer material without removal of material. The total volume removed is the sum of the volumes removed by all the asperities in contact with the polymer and can be expressed as

$$V = \frac{KW\ell \tan \theta}{p}$$

where V is the total volumetric wear, W is the total normal load, and $\tan \theta$ is the average asperity slope.

A correlation between the slopes of the asperities and the wear on the first pass can be seen in Table 4. For the ground and lapped surfaces the sliding direction periodically changes from parallel to perpendicular to the lay. Thus the average of the 90° and 0° slopes given in Table 3 has been tabulated in Table 4.

Table 4

Initial Mass Transfer as a Function of Average Asperity Slopes

<u>Surface</u>	<u>Average Slope</u>	<u>Mass Transferred (μg)</u>
Glass Bead Blasted	.1348	8.0
Surface Ground, Rough	.1033	4.62
Surface Ground, Smooth	.023	0.42
Hand Lapped	.0175	0.59

It is evident from Figure 2 and Table 4 that the initial mass transferred correlates both with the AA roughness and the average asperity slopes. However, the average slope is directly related to the mechanism of transfer and hence has a physical significance in this wear process.

As the plastic pin wears, two important geometric changes occur: the plastic material transferred to the metal surface changes the profile of the metal and a flat is worn on the surface of the pin. The transfer of the material to the surface does not occur as a continuous film as has been observed for plastics such as PTFE and linear high density polyethylene sliding on smooth surfaces [7]. Rather, it occurs in discrete lumps at widely separated asperities on the metal surface as shown in Figure 5. Since transfer as a result of abrasive wear will occur where the highest asperities contact the plastic surface, the surface parameters which describe these highest asperities would be the most relevant to predicting the plastic wear. Thus, it would be more appropriate to take the profile data and calculate statistics such as the slope and curvature of the upper most portions of the profile rather than from the complete profile as is common practice. The importance of the geometry of the asperity tips has been noted by Hollander and Lancaster [3]. They found an inverse power relation between polymer wear rates and the average radius of curvature of metal asperities.

As the plastic pin makes multiple passes on the same wear track, polymer continues to transfer but at a decreasing rate for the rougher surfaces (see Figure 2). The increase in the frequency of the deposits and the growth of the material transferred on previous passes on the ground surface is clearly shown in Figure 6. However, the transfer of polymer to the glass-bead blasted surfaces (Figure 7) occurs at asperities which are much more widely separated than those on the ground surfaces (compare Figures 6a and 7b, for example). As polymer builds up at the asperities, some of the normal load is supported by the polymer, resulting in less penetration of the steel asperities into the polymer surface. This decrease in penetration leads to a decrease in the wear rate.

The geometric characteristic of the surface which determines the amount of polymer which can be transferred to the surface is the volume of the valleys between the asperities. Surfaces with widely spaced peaks and

deep valleys will be able to be filled with more polymer than surfaces with close spaced peaks and shallow valleys. The AA roughness is a measure of the profile height distribution or of the depth of the valleys. The correlation length is a measure of the spacing between the asperities. The product of these two measures will be a parameter which is related to the volume of the valleys. The larger this product, the more polymer will be transferred to the surface. Table 5 indicates that a strong positive correlation exists between the product of AA roughness and correlation length and the wear after 40 passes.

Table 5
Correlation of Surface Parameters with Wear After 40 Passes

Surface	AA μm	Correlation Length, L, μm	AAxL μm^2	Wear μm
Glass Bead Blasted	1.26	34.2	43.1	39.3
Surface Ground	0.68*	17.1*	11.7	15.5
Surface Ground	0.135*	15.2*	2.9	3.3
Hand Lapped	0.067*	15.2*	1.0	2.3

* Measured perpendicular to the lay.

The friction force between two sliding surfaces involves two main components [2]: the rupture of junctions produced by adhesive forces at the contact point and the deformation of material by the relative motion of interlocking or interpenetrating asperities. In the wear of polymers both components are significant. For the initial passes of PCTFE sliding on steel surfaces, the location of the transferred polymer at asperities supports the deformation component as the dominant factor in the friction process (see Figure 5). A positive correlation between friction coefficient on the first pass and the AA roughness is indicated in Table 2. The coefficient of friction also correlates positively with the average slope.

However, it is evident that trying to predict friction of the polymer by parameters calculated from the entire profile is unrealistic in view of the limited portion of the metal surface in contact with the polymer. Hence, meaningful parameters would be those calculated from the upper portions of the profile.

The coefficient of friction of PCTFE on itself is reported as 0.27 for crystalline polymer rubbing against amorphous polymer [8]. On the rougher surfaces, the deformation component of the friction force is dominant during initial passes, giving coefficients of friction of .29 to .34. As the polymer transferred to the steel surface, more of the load was carried by a polymer-polymer interface and the friction coefficient was largely a result of polymer rubbing on polymer. Because the initial friction due

to deformation and the later friction due to polymer sliding on polymer were approximately equal, little change was observed on the coefficient of friction during a run.

On the smoother metal surfaces, the friction coefficient increased as the number of passes increased (Figure 3). The initial friction was low because the asperities were much smaller than those on the rougher surfaces. The smaller asperities did not penetrate as deeply as those on the rougher surfaces. As polymer transferred to the steel and more of the load was transferred to the polymer-polymer interface, the coefficient of friction rose approaching that of the polymer-on-polymer sliding system.

The change in the coefficient of friction as a result of transferred polymer is also shown in Figure 4. Initially the coefficient of friction when traveling parallel to the lay was less than that when traveling perpendicular to the lay. As polymer was transferred, the minimum friction was increased and the maximum decreased. These changes were due to the increasing dominance of the friction force by the polymer-polymer interface as the number of repeated passes increased.

CONCLUSIONS

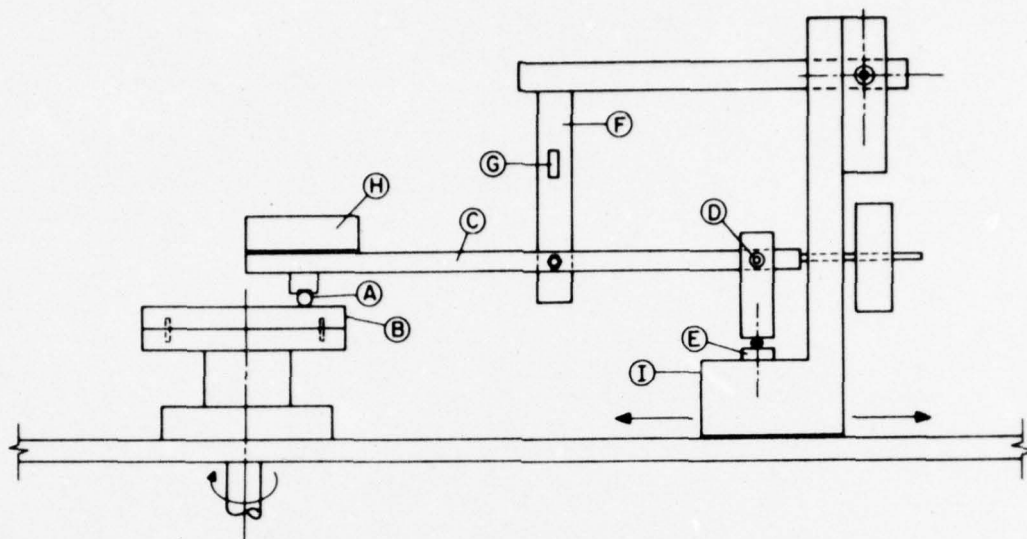
1. While AA roughness may correlate with friction and wear of plastics rubbing on hard surfaces, other parameters calculated from profile statistics such as asperity slope, and the product of the AA roughness and the correlation length also correlate and have a physical relationship to the friction and wear phenomena.
2. Because friction and wear phenomena involve the uppermost parts of a surface, some profile statistics (such as curvature, average slope, and wavelength) should be calculated for only the upper portions of the profile, if meaningful correlations are to be made.
3. On the initial pass of PCTFE on a mild steel surface, the friction and wear are dominated by deformation processes which are very dependent on the steel surface profile. On subsequent passes, as more polymer is transferred to the steel surface, the friction and wear are increasingly influenced by the interactions at the polymer-polymer interface.

ACKNOWLEDGEMENTS

This work was supported by a grant from the U.S. Army Research Office, Durham, North Carolina as a part of a continuing study on the transfer wear of polymers. The authors thank Mr. Clayton Teague and Dr. Russell Young of the Optics and Micrometrology Section of the National Bureau of Standards, Washington, D.C. for their assistance in measuring the surface profiles and calculating profile statistics and in generally encouraging studies which relate surface parameters to physical phenomena. One of us (NSE) also thanks Mr. H. T. McAdams, Calspan Corporation, Buffalo, N.Y. for his helpful discussions on profilometry and surface characterization.

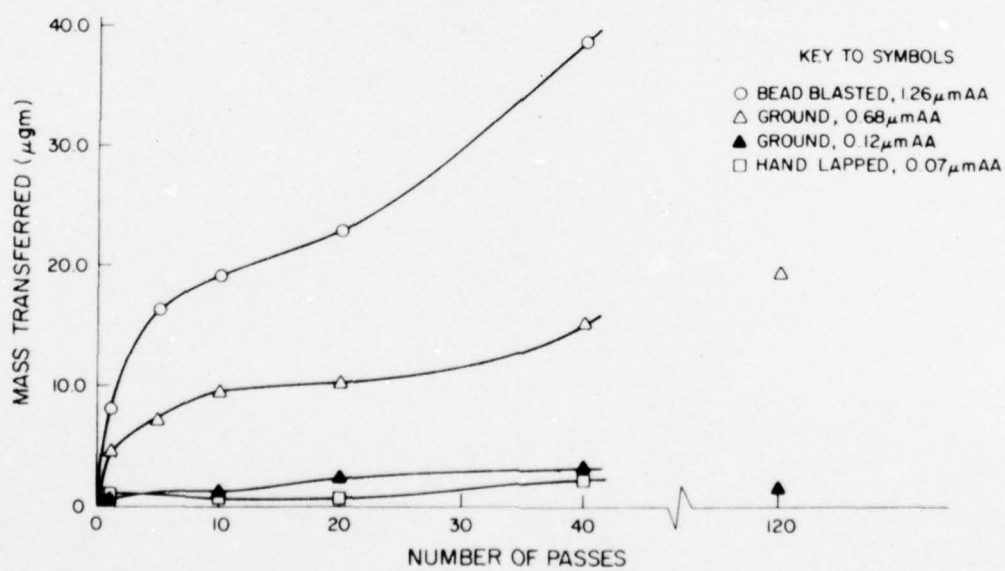
REFERENCES

1. Steijn, R. P., "Friction and Wear of Polymers," Metals Engineering Quarterly, ASM, 7, 9-21 (May 1967).
2. Lancaster, J. K., "Basic Mechanisms of Friction and Wear of Polymers," Plastics and Polymers, 41, 297-306 (December 1973).
3. Hollander, A. E., and J. K. Lancaster, "An Application of Topographical Analysis to the Wear of Polymers," Wear, 25, 155 (1973).
4. Young, R. D., and E. C. Teague, "The Measurement and Characterization of Surface Finish," (to be published).
5. Eiss, N. S., Jr., et al., (to be published).
6. Rabinowicz, E., Friction and Wear of Materials, John Wiley and Sons, 168 (1965).
7. Pooley, C. M., and D. Tabor, "Transfer of PTFE and Related Polymers in a Sliding Experiment," Nature Physical Science, 237, 88 [9](1972).
8. Anon., "Physical Properties of KEL-F 81 Plastic" Technical Information Bulletin, 3 M Company (August 1, 1961).



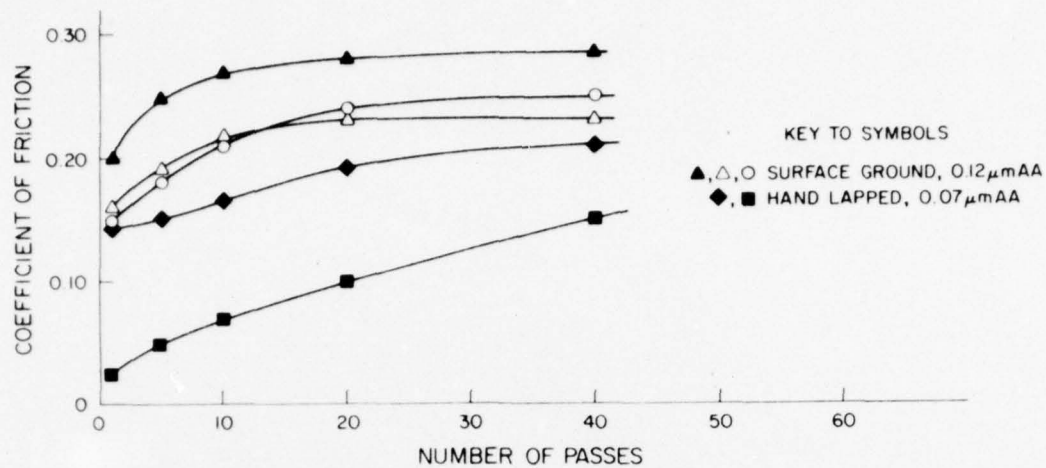
PIN-ON-DISK MACHINE

FIGURE 1



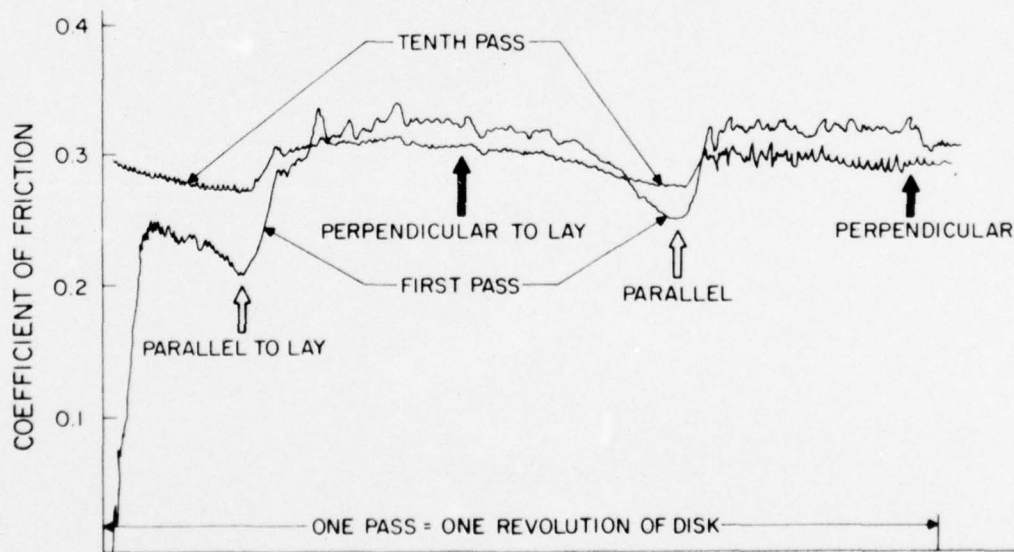
MASS TRANSFER OF PCTFE TO 1018 STEEL FOR VARIOUS SURFACE FINISHES AND NUMBER OF PASSES.

FIGURE 2



COEFFICIENT OF FRICTION OF PCTFE ON 1018 STEEL FOR GROUND AND LAPPED SURFACES AT VARIOUS NUMBERS OF PASSES DURING A 40 PASS RUN

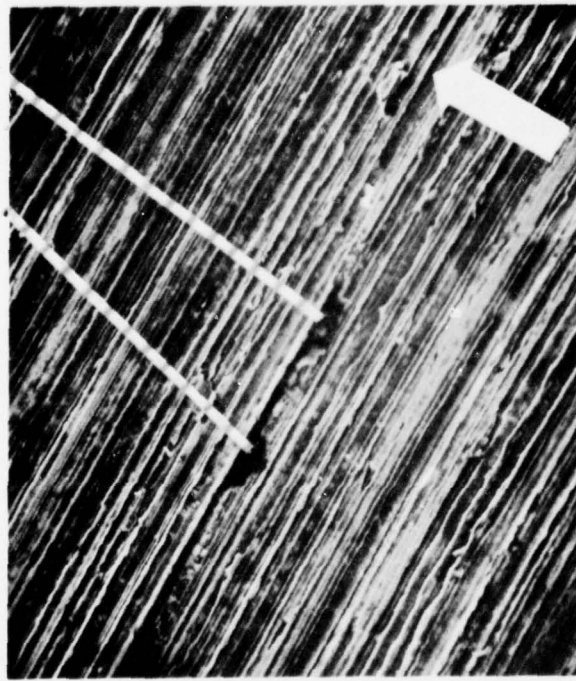
FIGURE 3



COEFFICIENT OF FRICTION FOR SURFACE GROUND 0.68 μmAA 1018 STEEL FOR FIRST AND TENTH PASS SHOWING INFLUENCE OF SLIDING DIRECTION - LAY ORIENTATION.

FIGURE 4

POLYMER DEPOSITS



50 μ

SLIDING
DIRECTION

(a) GROUND, 0.70 μ m AA

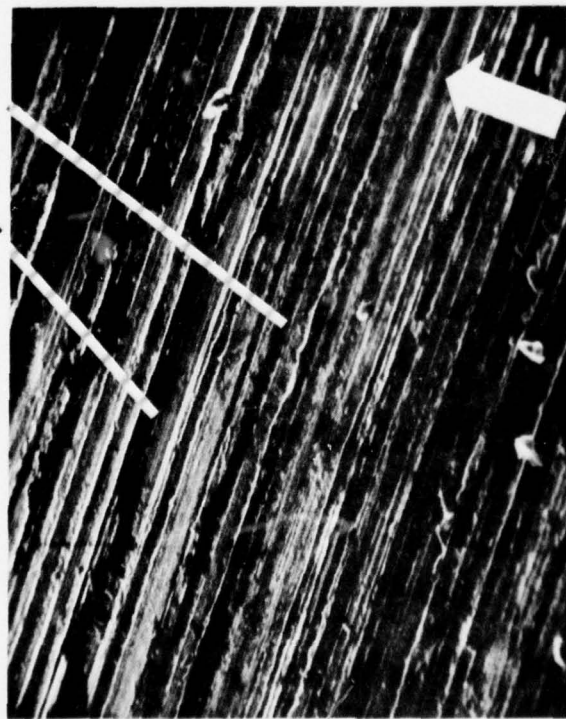


50 μ

(b) HAND LAPPED, 0.006 μ m AA

FIGURE 5. Initial transfer of PCTFE to steel surfaces.

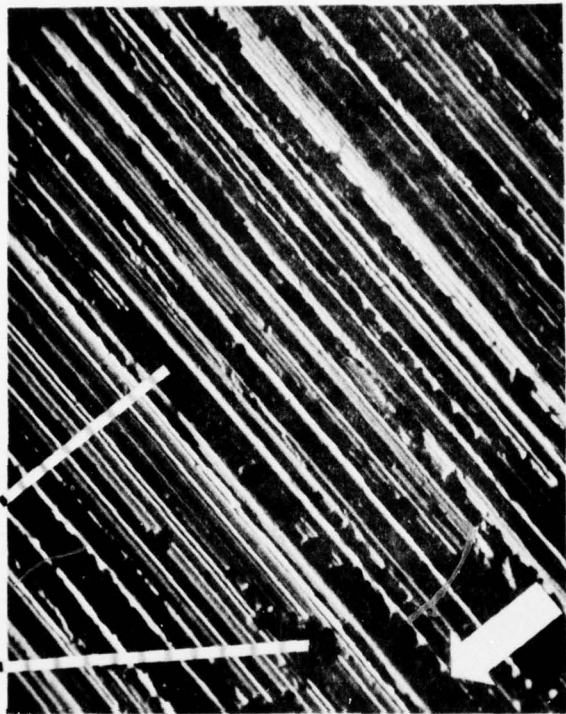
POLYMER DEPOSITS



50 μ

SLIDING
DIRECTION

(a) 40 PASSES



50 μ

(b) 120 PASSES

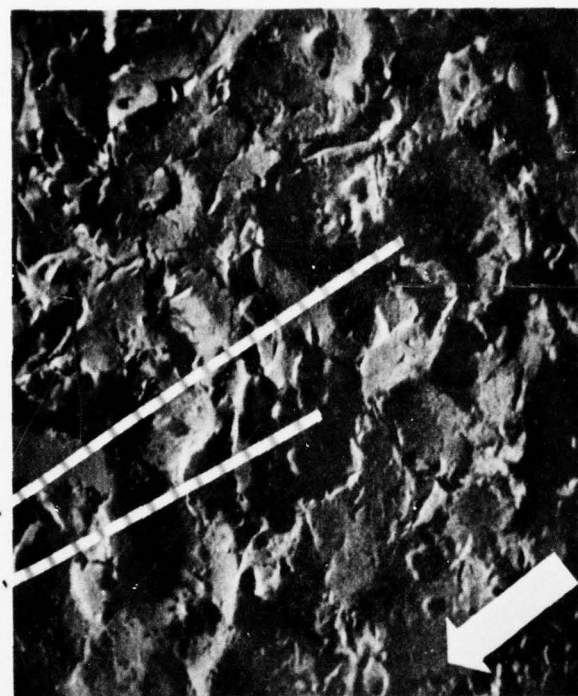
FIGURE 6. Transfer of PCTFE to 0.70 μ m AA steel surfaces.

POLYMER DEPOSITS



50μ

SLIDING
DIRECTION



50μ

(a) 5 PASSES

(b) 40 PASSES

FIGURE 7. Transfer of PCTFE to glass-bead blasted surfaces $1.2\mu\text{m AA}$.

APPENDIX 2

On the influence of the degree of crystallinity of PCTFE
on its transfer to steel surfaces of different roughnesses

N.S. Eiss, Jr. and J.H. Warren
Virginia Polytechnic Institute and State University
Blacksburg, Virginia

T.F.J. Quinn
University of Aston in Birmingham, England

presented
at the
Leeds-Lyon Symposium
on
Friction and Wear of Non-Metallic Materials
7-10 September 1976
Leeds, England

On the influence of the degree of crystallinity of PCTFE on its transfer to steel surfaces of difference roughnesses

N. S. Eiss, Jr. and J. H. Warren
Mechanical Engineering
Virginia Polytechnic Institute and State University
Blacksburg, Virginia - USA

T. F. J. Quinn
University of Aston
Birmingham, England

In this study, the wear of PCTFE on mild steel was measured using neutron activation analysis. The major variables studied were the crystallinity of the PCTFE and the roughness and lay of the steel counterface. Two degrees of crystallinity, 45 and 65 percent, were obtained by heat treatment. Surfaces were produced for the pin-on-disk apparatus by surface grinding to roughnesses ranging from 1.26 μm to 0.07 μm R_a and various lays. Wear measurements and SEM observations indicated that the crystalline polymer had higher wear than the amorphous polymer; the wear correlated with the inverse of the energy to rupture. The wear was highest when the direction of sliding was at an angle of 10 to 80 degrees to the lay for multiple passes over the same track. Under this condition, transferred particles of PCTFE were dragged out of the groove by the sliding motion leaving space for continued transfer to occur.

1. INTRODUCTION

When a polymer slides on a hard smooth surface, polymer transfers by two mechanisms. For PTFE and high density polyethylene, a very thin, highly oriented film transfers. Transfer is caused by adhesive forces

drawing out polymer molecules which can slide easily by each other because of their smooth molecular profile[1].^{*} When other polymers rub on the smooth surface, either no detectable film is transferred or transfer occurs in discrete lumps. The lump transfer is caused by the bulky side groups on the polymer chains inhibiting interchain movement and promoting fracture on a crystalline scale rather than molecular scale.

When a polymer slides on a rough surface, the mode of transfer is a lumpy transfer as a result of the abrasive wear mechanism[2]. Simple models of abrasive wear have related the wear directly to normal load, sliding distance, and average asperity slopes and inversely to the polymer hardness[3]. However, measurements of the wear of polymers making single traversals on steel surfaces at low speed did not confirm the proportionality between wear and asperity slope. Neither did wear of polymers correlate with the inverse of the polymer hardness.

Ratner[4] considers that work required to rupture the material during sliding, which is equivalent to the area under the stress-strain curve, is the most important parameter in abrasive wear of polymers. The work of rupture can be approximated by the product of the strain ϵ and stress S at rupture. Ratner found a correlation between wear rate and $1/S\epsilon$ of 18 polymers making single traversals on a $1.2 \mu\text{m } R_a^{**}$ steel surface.

When a polymer rubs on a rough surface for multiple passes, the wear rate is highest on the initial pass and decreases on subsequent passes[5]. One explanation for the decrease in wear rate is the increase in the load sharing by the transferred polymer which decreases the load supported

^{*} Numbers in brackets refer to literature listed in References.

^{**} R_a is the international symbol for arithmetic average roughness which has also been designated CLA and AA.

by the metal asperities. For smooth surfaces, the wear rate dropped to zero after a very few number of passes. For rougher surfaces the wear rate decreased with increasing passes but it was not conclusive that the wear rate would eventually reach zero.

In most work reported on the wear of polymers, little information is given to characterize the polymer. The method of polymer processing can result in a wide range of properties caused by different degrees of crystallization and different crystal habits. Mechanical properties are also highly influenced by the amount of plasticizers used in the polymer.

In this paper the wear of the polymer polychlorotrifluoroethylene PCTFE will be examined as a function of the degree of crystallinity of the PCTFE, roughness and lay of the steel surfaces, and the number of repeated passes over the surface. The work extends the single traversal and limited multiple pass experiments to long run experiments with a polymer of different crystallinities.

2. EXPERIMENTAL

2.1 Apparatus

A pin-on-disk machine, shown in Fig. 1, was used to provide relative motion between the materials. The polymer pin, A, was mounted in arm, C, which pivoted vertically at D and horizontally at E. Horizontal motion of the beam was restrained by a cantilever beam, F, on which were mounted strain gauges, G. The output of the strain gauges was plotted on an X-Y recorder and calibrated to read friction force. The normal load was applied by dead weight, H. The disk rotation was controlled by a

variable speed transmission and the power was supplied by a 1/2 HP synchronous motor. The radius of the path of the pin on the disk was controlled by moving the pivot support, I, in the directions indicated.

The transfer of the polymer to the disk was measured by Neutron Activation Analysis (NAA), a technique which has been described in [6]. In these experiments, PCTFE was selected for the pin material because it contained chlorine which is suitable for NAA. However, the analysis of the amount of PCTFE transferred was performed differently from that described in [6]. Instead of measuring the activity of the Cl^{38} isotope through a window which spanned the two major energy peaks of gamma radiation, the activity of each energy peak was measured. The mass transferred was then calculated to be the average of the mass predicted by each energy peak.

2.2 Experimental Materials

The PCTFE pins were prepared from 3.18 mm dia extruded rod. Two degrees of crystallinity were obtained by a procedure obtained from the manufacturer of the polymer [7]. The PCTFE rod was inserted in a quartz tube with a 3.18 mm dia, placed in a furnace, and heated to 218 C. Following a half hour at that temperature, one set of samples was removed from the furnace and quenched in water. These samples had a lower degree of crystallinity and are designated as amorphous in this paper. A second set of samples remained in the furnace while it cooled down to 100 C over a one-hour period. These samples had a higher crystallinity and are designated as crystalline in this paper. The PCTFE rods were then cut to a length of 7.9 mm and turned to conical shape with a 20° half

angle on a lathe, washed in pentane, air dried, and sealed in polyethylene vials.

To obtain confirmation of the effect of heat treating the PCTFE, x-ray diffractions were obtained on the as-received extruded rod, and the amorphous and crystalline heat treated specimens. The specimens were sliced into 0.5 mm thick pieces for the flat-plate x-ray diffraction camera, or chopped into small particles for the cylindrical (powder) camera.

Each specimen was first irradiated with copper K α radiation, 1.54 \AA wavelength, λ , in the flat-plate camera, the specimen to plate distance, D, being maintained at 40 mm for each exposure. Diffraction rings will appear at angles 2θ from the original direction for crystalline specimens, the value of 2θ being related to the radii, R, of the rings by $R = D \tan 2\theta$. The Bragg Angle, θ , is given by $2 d \sin \theta = \lambda$ where d is the interplanar spacing.

Powdered specimens were placed on a glass fiber and irradiated with Cu K α radiation. The diffraction maxima were recorded on a cylindrical film placed 5.73 cm from the fiber axis. Thus, the distance along the film from the undeviated direction when measured in millimeters, will also be the value of 2θ in circular measure.

The disks were machined from 1018 cold rolled steel bar. The surfaces of the disks on which the pin rubbed were ground with roughnesses and lays shown in Table 1. Disks with a unidirectional lay were ground on a surface grinder. The radial and circular lays were ground on a lathe. The radial lay was generated such that the lay in the vicinity of the

radii of the wear tracks was perpendicular to the sliding direction. After grinding, disks were coated with oil to retard rusting. Just prior to testing, the disks were repeatedly flooded with methanol and wiped with a paper wiper. A final thin coating of methanol was allowed to evaporate from the disk prior to the start of a run.

2.3 Experimental Procedure

All experiments were run at 0.49 N normal load and .935 cm/sec sliding speed in laboratory air at an average temperature of 24 C and relative humidity of 60%. A typical run would start with irradiation of the PCTFE pin in the reactor for 10 minutes. The pin was then mounted in the holder and the disk rotated. At 50, 100, 250, 500, 750 and 1000 revolutions, the disk was removed, the radioactivity counted, and then the disk was returned to the apparatus to continue the run. Two tracks were run on each unidirectionally ground disk at 14.3 mm and 16.8 mm radius. The NAA was calibrated by placing known masses of PCTFE at these radii on the disks and measuring the activity.

To obtain a measure of the uniformity of transfer to a disk with unidirectional lay an autoradiograph was made by placing a disk with transferred PCTFE on high resolution medical x-ray film for one hour. The disk had made 200 revolutions when the autoradiograph was made.

3. RESULTS

3.1 Degree of Crystallinity of PCTFE

In general, the flat plate photographs from the extruded rod and the amorphous and crystalline structures revealed more information than the

diffraction patterns obtained in the cylindrical camera. In particular, preferred orientation effects can only be observed in the flat plate photographs because the specimens must be ground up before irradiating in the cylindrical camera. Table 2 gives the interplanar spacings and descriptions of the diffraction maxima.

3.2 Effect of Crystallinity on Polymer Transfer

The effect of the heat treatment on the polymer transfer is shown in Fig. 2. Two runs were made on each disk, one with an amorphous pin and one with a crystalline pin. Because the runs were made at different radii on the disk, one revolution of the disk (pass) resulted in a different sliding distance for each run. The mass transferred to the disks was normalized by the track circumference which is expressed in units of m/pass. Thus the wear is reported in kg-pass/m. The data is plotted as a function of the number of passes rather than the sliding distance because in multiple pass experiments the transfer which occurs each pass is influenced by the material transferred on previous passes. In a study of the transfer during the first and subsequent passes [5] it was convenient to plot the data as a function of the number of passes and this abscissa for the plots has been continued in this research.

From the data in Fig. 2a, the mass rate transferred was calculated and plotted in Fig. 2b. Comparing the wear rates of the crystalline and amorphous pins on the same disks, it is seen that in all comparisons except at 375 passes on disk A, the wear rate of the crystalline pin was greater than that for the amorphous pin. Fig. 3 shows the mass transfer on two disks which were smoother than those used in the runs plotted in

Fig. 2. Of the seven comparisons of the wear of crystalline and amorphous pin on the same disk, the transfer of crystalline PCTFE was greater than that for the amorphous PCTFE in four comparisons.

3.3 Effect of Roughness on Polymer Transfer

Figs. 2a and 3 illustrate the effect of roughness as measured by the arithmetic average R_a . The mass transfer on the smoother surfaces is an order of magnitude less than that for the rough surfaces. It was also noted that the wear on the rough surfaces continued throughout the experiment run whereas most of the wear on the smooth surfaces occurred in the first few passes. Because of the lesser amount of transferred material on the smooth surfaces, the radioactivity of the Cl^{38} had become indistinguishable from the background for runs greater than 250 passes.

The data shown in Figs. 2 and 3 were obtained on disks which were unidirectionally ground. A circular wear track on the disk would result in the sliding vector rotating 360° with respect to the lay during one revolution of the disk. Hence, a roughness parameter measured perpendicular to the lay would not be indicative of the composite roughness seen by the pin during a revolution. Disks were ground with a radial lay and a circular lay so that wear could be obtained on a disk for which the roughness measure would apply to the entire circumference on the wear track. These wear data are shown in Fig. 4.

The data shows that the transfer of an amorphous pin to the rougher of the two radial ground disks was greater than that of the crystalline pin to the smoother surface. Here the greater roughness of disk M completely masked the difference in wear of amorphous and crystalline

PCTFE observed on the unidirectionally ground disks. Comparing Fig. 4 with Fig. 2 shows that comparable wear was obtained even though the roughness of the radial ground disks was 3 to 4 times that of the unidirectionally ground disks. Comparing Fig. 4 with Fig. 2 shows that comparable wear was obtained even though the roughness of the radial ground disks was 3 to 4 times that of the unidirectionally ground disks. Clearly the difference in lay had an influence on the transfer; this effect will be discussed later.

The transfer of the polymer to the disks with circular lay was four to five times less than the transfer to unidirectional ground disks of comparable roughness (Compare Figs. 4 and 2a). While lay is also a factor in the comparison, another factor is the roughness measurement on the circular lay. Because the stylus instrument moved in a straight line, it did not track along the circular grooves. Hence, the stylus measured a component of roughness perpendicular to the grooves which gave a reading higher than if the stylus tracked in the grooves. Because the wear track followed the circular lay, the roughness that the polymer responded to was less than that traversed by the stylus. In comparing Figs. 3 and 4 it is noted that the wear on the smooth unidirectional ground surfaces was comparable with that on the circular lay disks.

4. DISCUSSION

4.1 Degree of Crystallinity

The most significant result of the x-ray investigation of the structure of PCTFE is the preferred orientation which exists in the

extruded rod. Evidence for this orientation is the arcs observed in the photos taken by the flat-plate camera which are noted in Table 2. The absence of arcs in either of the other specimens indicates the removal of the preferred orientation by the heat treatment. No arcs were observed in the cylindrical powder camera results on the extruded rod because it is chopped up into a powder which destroys the orientation. Preliminary wear experiments with the extruded rod showed that the wear rate was higher when sliding parallel to the rod axis than when sliding on the end of the rod with the axis perpendicular to the surface. These preliminary experiments agree with the x-ray data.

Both the flat plate and cylindrical camera techniques reveal that the crystalline specimens have very prominent interplanar spacings at 5.75 and 5.44 Å. These spacings also appear to be present in the extruded rod (see 5.53 Å which could be a doublet). It is possible that these spacings are related to the helical structure of the PCTFE. According to Kaufman[8] the repeat distance of the helical structure is 35 Å, while Liang and Krim[9] maintain it is 43 Å. These investigators assumed 13 and 16 monomer units of 2.69 Å, respectively. If the repeat distance 43 Å is divided by the 5.44 Å spacing, the result 7.9 is approximately half of 16 repeat units of 2.69 Å. Hence, this spacing may be an indication of the helix structure. However, considerably more work is required to relate the spacings to the polymer structure.

The data in Table 2 show that more sharp lines are present in the crystalline than in the amorphous patterns. These sharp lines also indicate a higher degree of crystallinity. The manufacturer of this polymer states that these heat treatments should yield structures which are about

45 percent crystalline for the amorphous (quenched) and 65 percent for the crystalline (slow cooled). The manufacturer also indicated that the degree of crystallinity could be predicted from the following relation[7]:

$$\text{Percent crystallinity} = 1503 - (3067/\text{specific gravity})$$

However, the specific gravities for 45 and 65 percent are 2.104 and 2.133, respectively. Hence, to predict percent crystallinity by this equation, one would have to measure the specific gravity to a minimum of three significant figures and preferably to four. While an attempt was made to measure the specific gravity it was limited by the accuracy of the measurement of the volume of the specimen. A technique for measuring specific volume by measuring buoyancy is described in [10].

4.2 Effect of Crystallinity on Wear

One of the effects of the different heat treatments is to alter the mechanical properties of the polymer as shown in Table 3. If the Se products for the amorphous and crystalline PCTFE are compared, the crystalline polymer should wear more [4] which was confirmed by the data shown in Fig. 2.

The difference in both the amount and size of the particles transferred to the steel were confirmed by scanning electron microscope (SEM) photographs. Fig. 5 shows that more crystalline PCTFE is on the disk than amorphous PCTFE. In addition, the loose wear particles at the edge of the wear track were more numerous for the crystalline material than for the amorphous.

4.3 Effect of Roughness and Lay on Wear

Lancaster[3] shows that roughness as measured by R_a has a strong positive correlation with the abrasive wear of polymers making single traversals of polymers over steel at low speeds. A comparison of Fig. 2 and 3 shows that this correlation also holds for multiple pass experiments. However, the roughness effect interacts with the lay of the surface in determining abrasive wear and hence both parameters must be considered.

Fig. 6 is an SEM photo of a wear track on a unidirectionally ground disk. As the sliding direction changes with respect to the lay of the surface, the loose particles which are on the inside of the track in the left side of the photo are not present when the sliding vector is parallel to the lay. The loose particles are on the outside of the track in the right side of the photo. The photo also indicates that there is more transfer when the sliding direction is at an angle to the lay than when it is parallel to the lay.

Confirmation of this non-uniform transfer as a function of sliding-to-lay directions is shown in the autoradiograph of the wear tracks in Fig. 7. The darkest portions of the track, which indicate the greatest transfer, occur when the sliding velocity is at an angle of 10 to 80 degrees to the lay. The transfer is least when sliding parallel to the lay and intermediate when sliding perpendicular to the lay.

One of the objectives of this work was to see if the transfer of PCTFE to the steel would reach an equilibrium state at which the transfer would cease after multiple passes. The data in Fig. 2 indicated that only one run out of four appears to be approaching such an equilibrium. The others show little evidence of reaching equilibrium after 750

passes. The mode of wear that occurs when the sliding direction makes an angle with the lay provides an explanation for not reaching equilibrium. As abrasive wear occurs, particles of polymer transfer to the steel surface. On subsequent passes, the friction of the passing polymer pin moves the transferred material along the grooves until it emerges at the edge of the track where it accumulates. Because the polymer is continually being moved out of the groove, more space is available for polymer to be transferred and the wear will continue. However, when the polymer slides either parallel to or perpendicular to the lay, transferred material can not move to the edge of the track. It can only be pulled along or over the asperities into the next groove and hence the transfer that can occur is limited by the volume of grooves between the surface of the steel and that of the polymer pin.

To test the limiting nature of transfer when sliding parallel to and perpendicular to the lay, the radial ground and circular grooved disks were prepared. As the radial lay disks used in these tests were the first ones produced with this radial grinding technique, the roughness was difficult to control. As a consequence they were much rougher than the unidirectional lay disks. The large roughness was due in part to some extremely high ridges such as the one shown in Fig. 8(a). Hence, an equilibrium state of no wear was not achieved as expected because the high ridge continued to remove polymer on each pass. It is important to note that the wear on the radial lay disks is comparable with that on the unidirectional lay disks in spite of the much higher roughness of the radial lay disks. Hence, a more uniform roughness on a radial lay disk would give less wear and approach an equilibrium state.

Fig. 8 shows the fine wear debris from the crystalline pins and the lumpier, large debris from the amorphous material found on the radial lay disks. The crystalline material, being slightly more brittle than the amorphous material, has less elongation to rupture and hence produces smaller wear particles as observed.

5. CONCLUSIONS

The x-ray data on the extruded rod and heat treated PCTFE show that a wide variety of structural configurations are possible for a given polymer. Because the structure determines mechanical properties, prediction of abrasive wear which is a strong function of mechanical properties depends on knowing the polymer structure. The structure of PCTFE which is less crystalline has a larger energy to rupture and lower wear than the more crystalline specimens.

The achievement of an equilibrium transfer condition is a strong function of the direction of sliding with respect to the surface lay. Multiple pass experiments, sliding either parallel to or perpendicular to the lay, result in the grooves filling up with transferred polymer. The transferred polymer shares some of the normal load, and eventually reduces the transfer rate to an insignificant value. When sliding occurs at an angle to the lay, the transferred polymer is gradually moved out of the grooves providing room for more transferred polymer. Hence, wear continues indefinitely.

It is evident that characterizing the roughness of a surface is often insufficient if polymer transfer is to be predicted. The interaction between roughness and lay is significant and must be considered.

6. ACKNOWLEDGEMENTS

This work was sponsored by the Army Research Office, Research Triangle Park, North Carolina as a portion of a study on the transfer wear of polymers. The x-ray analysis was performed in the laboratories of the physics department, University of Aston, Birmingham. The autoradiographs were made and processed in the Plant Pathology Laboratory, V.P.I. and S.U. with the advice and assistance of Dr. S. W. Bingham. The assistance and cooperation of the personnel of the Neutron Activation Analysis Laboratory at V.P.I. and S.U. for providing space for the apparatus as well as assistance in interpreting data is gratefully acknowledged.

REFERENCES

1. Briscoe, B. J., Pooley, C. M., and Tabor, D. 'The Friction and Transfer of Some Polymers in Unlubricated Sliding.' 'Advances in Polymer Friction and Wear.' 1974 Ed. Lieng-Huang Lee (Plenum Press, New York) 191-204
2. Lancaster, J. K. 'Basic mechanisms of friction and wear of polymers.' *Plastics and Polymers*, Dec. 1973, 41, 297-306
3. Rabinowicz, E. 'Friction and Wear of Materials' 1965 (John Wiley and Sons, New York) p. 168
4. Ratner, S. B., Farberova, I. I., Radynbeovich, O. V. and Lur'e, E. G. 'Connection between wear resistance of plastics and other mechanical properties' 'Abrasion of Rubber' 1967 Ed. D. I. James (MacLaren & Sons, London) p. 145
5. Eiss, N. S. Jr. and Warren, J. H. 'The Effect of Surface Finish on the Friction and Wear of PCTFE Plastic on Mild Steel.' *Soc. Manu. Eng.* Paper No. IQ75-125, April 1975
6. Eiss, N. S. Jr., Doolittle, S. D. and Warren, J. H. 'An Application of Neutron Activation Analysis to the Measurement of the Wear of Polymers' *Wear*, 1976, 38, 1, 129-143
7. 'Physical Properties of KEL-F 81 Plastic' *Tech. Info. Bull.*, 3M Company, August 1, 1961
8. Kaufman, H. S. 'X-Ray Examination of Polychlorotrifluoroethylene.' *J. Am. Chem. Soc.*, 1953, 75, 1477
9. Liang, C. Y. and Krimm, S. 'Infrared Spectra of High Polymers. III. Polytetrafluoroethylene and Polychlorotrifluoroethylene.' *J. Chem. Phys.*, 1956, 25, 563
10. Hoffman, J. D. and Weeks, J. J. 'Specific Volume and Degree of Crystallinity of Semicrystalline Poly(chlorotrifluoroethylene), and Estimated Specific Volumes of the Pure Amorphous and Crystalline Phases.' *Jl. Res. Nat. Bur. Standards*, May 1958, 60, 5, 465-479

Table 1. Surface Characterization of Disks

Disk	Roughness AA μm	Lay Description
A	0.63 [*]	Unidirectional
B	0.71 [*]	Unidirectional
F	0.13 [*]	Unidirectional
G	0.12 [*]	Unidirectional
M	2.30 [*]	Radial
N	2.71 [*]	Radial
O	0.59 ^{**}	Circular
P	0.77 ^{**}	Circular

^{*} measured perpendicular to lay

^{**} measured parallel to lay

Table 3. Mechanical Properties of PCTFE for Different Heat Treatments[7]

Property	Amorphous	Crystalline
Yield Strength	17.93 MN/m ²	23.1 MN/m ²
Tensile Strength(S)	36.27 MN/m ²	35.85 MN/m ²
Elongation to Break(e)	1.8 m/m	1.25 m/m
Product Se	65.3 MNm/m ³	44.8 MNm/m ³
Elastic Modulus	1.1 GN/m ²	1.31 GN/m ²

Table 2. Interplanar Spacings of PCTFE as Extruded and Heat Treated

Flat-Plate Camera		Cylindrical Powder Camera	
Extruded Rod			
d(Å)	Description of line	d(Å)	Description of line
5.48	Broad, strong line, Arcs at 0° and 180°	~15	Very broad, diffuse line of medium, uni- form intensity
3.30 } 2.85 }	Broad line, faint Arcs at 0° and 180°	5.53	Broad strong line of uniform intensity, possibly a doublet
2.71 } 2.33 }	Broad line, faint Arcs at 90° and 270°	4.03	Broad, diffuse, med- ium intensity
		2.31	Sharp, faint, uniform intensity
Amorphous			
5.86	Broad, strong line, uniform intensity	~12 } ~ 4 }	Very broad, diffuse lines, medium intensity
3.41 } 3.04 } 2.44 }	Broad, very faint, uniform lines	2.31	Sharp, faint line, uniform intensity
Crystalline			
5.75	Medium, strong line uniform intensity	~12	Broad, diffuse faint line, uniform intensity
5.48	Sharpline, medium uniform intensity	5.74 } 5.40 }	Broad, strong lines
3.30 } 2.84 }	Sharp, faint lines of uniform intensity	~4	Broad, diffuse, faint line
2.44	Broad, faint, uniform		

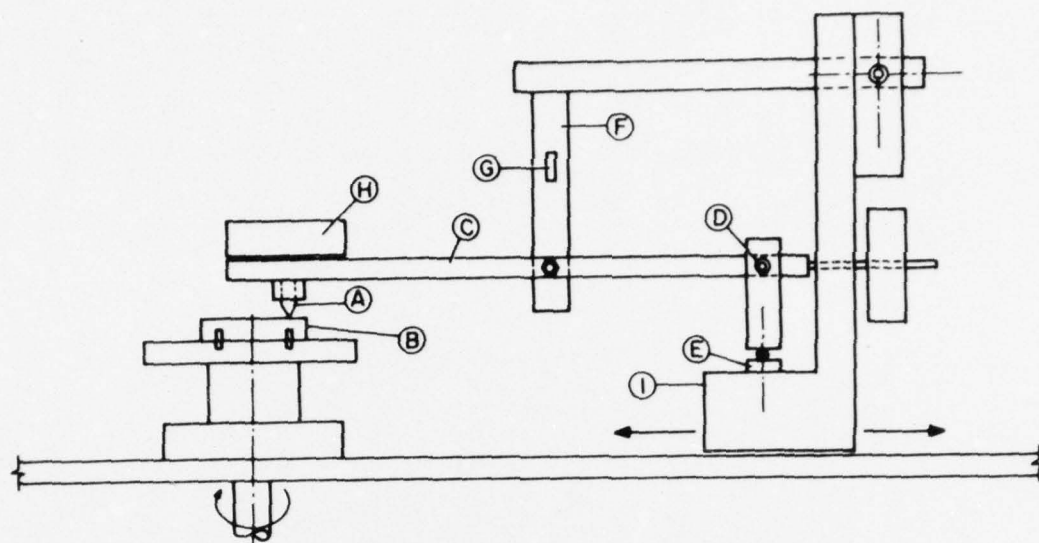


Fig. 1 Pin-on-Disk Machine

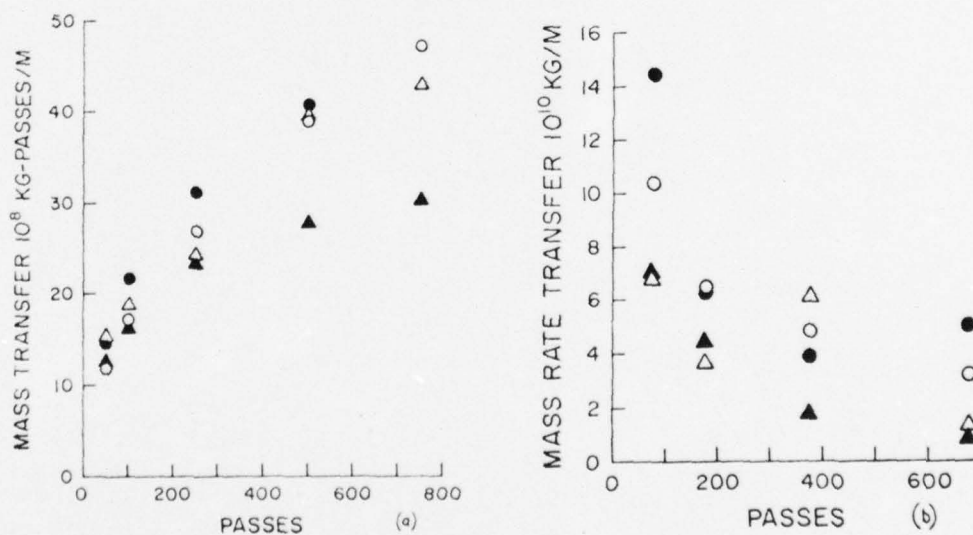


Fig. 2 Mass (a) and Mass Rate (b) Transfer as a function of the number of repeated Passes of a PCTFE pin on a 1018 steel surface. Load 0.49N, Sliding Speed 0.935 cm/sec;

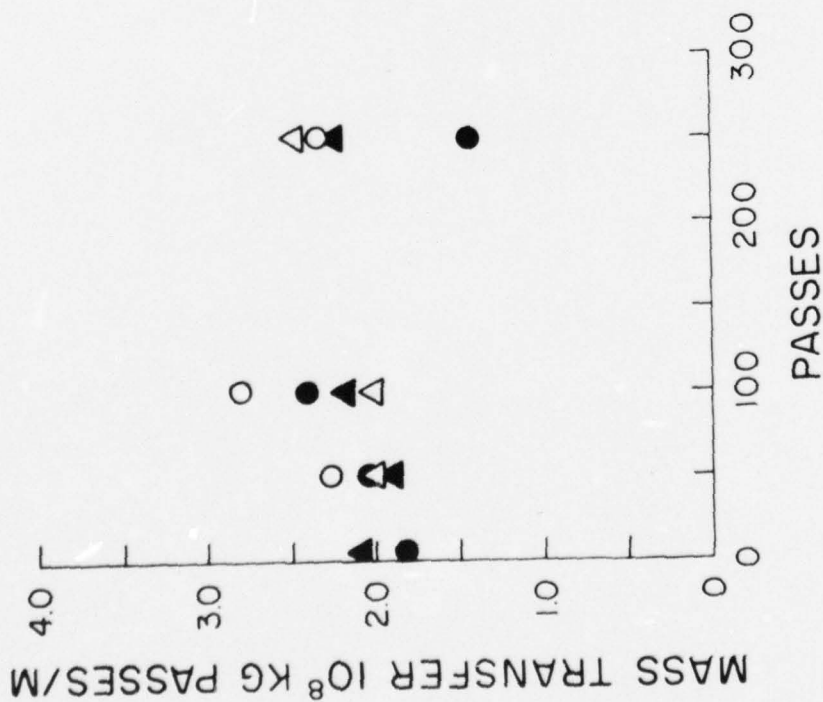


Fig. 3

Mass transfer as a function of the number of repeated passes of a PCTFE pin on a 1018 steel surface. Load 0.49N, Sliding Speed .935 cm/sec;

Disk F ○ - crystalline pin
 Disk G ● - amorphous pin
 Disk G ▲ - crystalline pin
 Disk G ▼ - amorphous pin

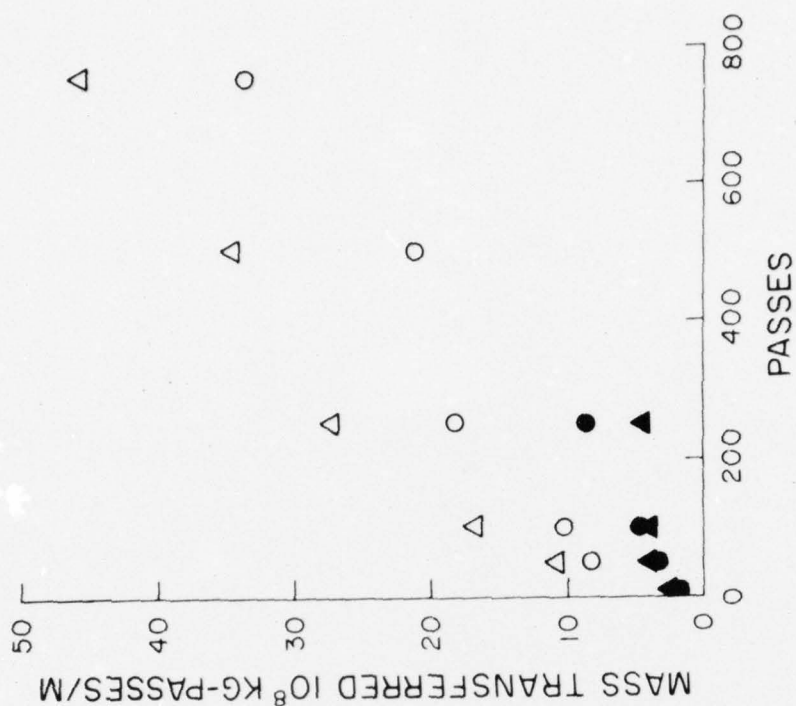


Fig. 4

Transfer of PCTFE to Radial and Circular Lay, 1018 steel disks. Load 0.49N, Speed .935 cm/sec;

Radial lay: ○ - crystalline pin, disk M
 Circular lay: ● - amorphous pin, disk N
 Radial lay: ▲ - crystalline pin, disk O
 Circular lay: ▼ - amorphous pin, disk P



0.1 mm

a



0.1 mm

b

Fig. 5 Transfer of PCTFE to Disk B. (a) Amorphous (b) Crystalline Load 0.49N, Speed 935 cm/sec, 1000 passes, arrows indicate slider motion.



Fig. 6 Variation of Transfer of PCTFE to steel as a function of the angle between the lay and the sliding direction. The wear track lies inside the deep reference groove which was scribed on the disk prior to transfer.

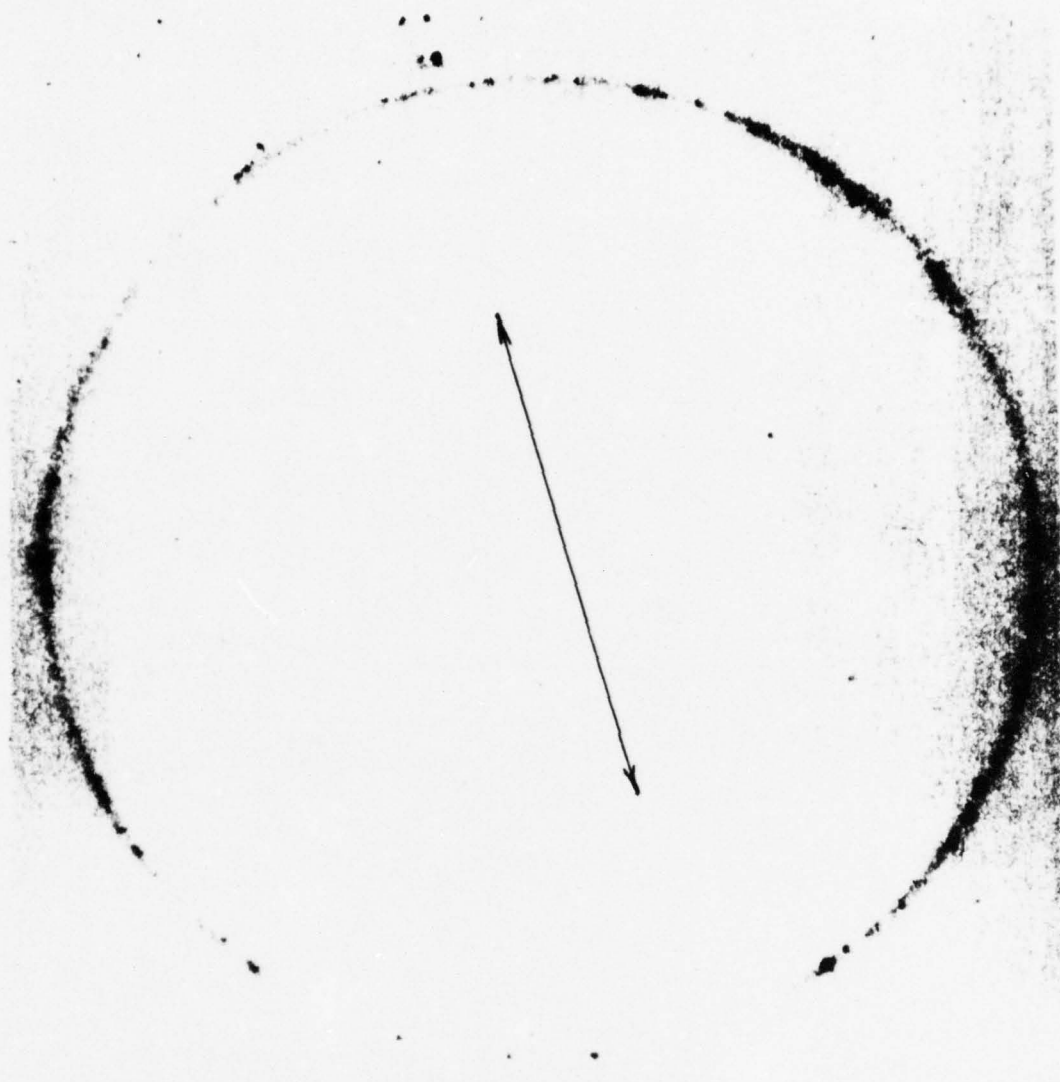


Fig. 7 Autoradiograph of transfer of PCTFE to steel disk,
Load 1.96N, Speed .935 cm/sec, 200 Passes. Arrow
indicates direction of lay.

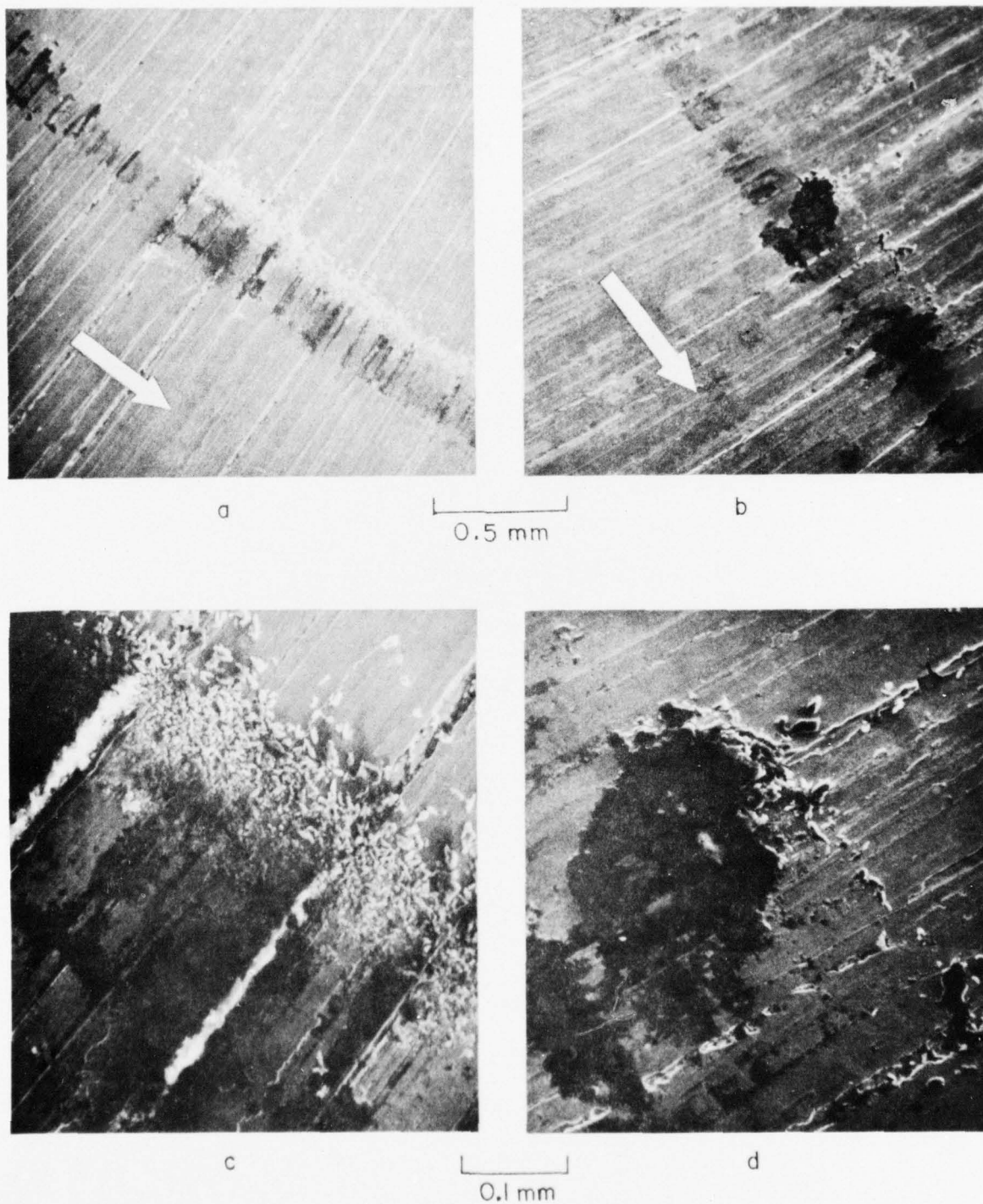


Fig. 8 Transfer of PCTFE to Surfaces with Radial Lay. Load 0.49N, Speed 935 cm/sec (a,c) crystalline pin on disk M (b,d) amorphous pin on disk N. Arrow indicates slider motion.

Contribution to the discussion of the paper by N.S. Eiss, J.H. Warren and T.F.J. Quinn entitled "On the Influence of the Degree of Crystallinity of PCTFE on its Transfer to Steel Surfaces of Different Roughnesses".

The authors have reported that further work to establish the structure of PCTFE in more detail might be of value in determining the mechanism of wear. I have carried out work in the last few months at Aston University which has shed some further light on this topic and which may be of interest.

X-ray diffraction pictures of a number of samples - worn, unworn, "amorphous" and "crystalline" - have been obtained using the conventional Powder Camera modified so that glancing angle photographs (as described by Isherwood & Quinn : Brit.J.Appl.Phys. 1967, 18, pp. 717-25) could be obtained. These pictures showed lines corresponding to two tetragonal forms of crystal. The larger unit cell ($a = 7.5 \text{ \AA}$; $c = 11.5 \text{ \AA}$) is perhaps more common in the "crystalline" samples, with a smaller cell ($a = 7.2 \text{ \AA}$; $c = 8.7 \text{ \AA}$) more common in the "amorphous" samples. The evidence shows quite clearly that the two forms exist, but, due to practical problems, intensity measurements have not so far been made which could confirm the proportions of the two types.

The larger cell contains seven monomeric units, whilst the smaller contains five monomeric units. Calculations based on atomic volumes show that each cell contains a single turn of a helix. These calculations were made on the assumption that the published S.G. of 2.12 could be applied to both cells. However, it is likely that the slight differences, which can be measured for different samples of the polymer, are due to different proportions of the two cell types, and that these have in fact slightly differing densities.

It may further be assumed that the three forms of polymer (atactic, isotactic and syndiotactic) will all settle down to one of these two forms, and that their existence represents slightly different energy levels. This being so, it is possible that the difference in wear between "amorphous" and "crystalline" samples may be explained by the presence of these different energy levels in different proportions. Wear, which requires the "teasing" apart of the crystallite structures, will then be reduced when the sample contains more of the low energy form.

C.J.L. Tye,
Dept. of Physics,
University of Aston in
Birmingham,
Birmingham B4 7ET.

14th September, 1976.

APPENDIX 3

Depth of Penetration as a Predictor of the Wear
of Polymers on Hard, Rough Surfaces¹

J. H. Warren, Graduate Research Assistant², Assoc. Mem. ASME

N. S. Eiss, Jr., Associate Professor, Mem. ASME

Virginia Polytechnic Institute and State University
Blacksburg, Virginia

to be presented at the

International Conference on
Wear of Materials, 1977

St. Louis, Missouri

April 26-28, 1977

ABSTRACT

Polymers were slid on rough, hard surfaces with normal loads which caused full penetration (real and apparent areas equal) and partial penetration (real less than apparent area). SEM photographs of full penetration showed that the polymer sheared off at an angle to the horizontal, the shear angles were 10.8, 12.6, and 18.9 deg for polyvinylchloride, polychlorotrifluoroethylene, and nylon 6/6, respectively. These shear angles correlated with the energy-to-rupture of the polymers and inversely with the wear of polyvinylchloride and polychlorotrifluoroethylene. In partial penetration experiments the wear of polyvinylchloride and polychlorotrifluoroethylene could be discriminated by the depth of penetration of the surface into the polymer. The penetration depth is a function of the polymer yield strength and the bearing area curve of the surface.

NOMENCLATURE

- A_r = Real area of contact (m^2)
- BC = Background Count
- n = Number of measurements
- PC = Peak Count
- PE = Percent Error = $100(BC + PC)^{0.5}/PC$
- R_a = Arithmetic average roughness (μm)
- RMS = Root mean square roughness (μm)
- s = Standard deviation of the shear angle (deg)
- W = Normal load (N)
- y = Yield Strength (MN/m^2)
- ϕ , ϕ_h , ϕ_l = Mean, high, and low shear angles, respectively (deg)

INTRODUCTION

The transfer of a polymer to a hard surface occurs in two modes. One mode is a thin film transfer on very smooth surfaces (less than $0.1 \mu m R_a$). This mode has only been observed for polytetrafluoroethylene, PTFE, and high density polyethylene,

HDPE (1).³ The other mode is lumpy transfer which has been observed both on smooth surfaces (2) and rough surfaces (1-3) for a variety of polymers. The thin film transfer has been explained by adhesive forces drawing out polymer molecules which can easily slide by each other because of their smooth molecular profile.

The transfer of polymer to rough surfaces has been shown experimentally to correlate positively with several parameters. Ratner (4) correlated wear rate of 18 polymers making a single transversal on a $1.2 \mu m R_a$ steel surface with the reciprocal of the product of the tensile strength and the elongation at rupture. Lancaster (5) showed non-linear but positive correlations of wear with the average asperity slope, R_a roughness, and the inverse of the polymer hardness. A simple model for abrasive wear (6) predicts that wear is proportional to the normal load, sliding distance, and average asperity slope and inversely proportional to the polymer hardness. These experimental results and abrasive wear model clearly show that both polymer mechanical properties and surface topography characterization are needed to make a quantitative abrasive wear model.

The simple abrasive wear model (6) is based on the assumption that all of the polymer in front of a penetrating asperity is removed when sliding occurs. However, if the asperity slope is extremely small it is possible that the asperity causes only elastic stresses in the polymer and sliding produces no permanent deformation or fracture of the polymer. Lancaster (5) calculated the limiting asperity slopes for the onset of plastic deformation when polymer asperities were flattened level with a base plane. He concluded that polymers are more likely to experience only elastic stresses at the asperity contacts than metals.

The calculations made by Lancaster imply that there is a critical asperity slope below which the stresses are insufficient to cause wear, this slope being a function of the ratio of the hardness to the elastic modulus for the polymer. A portion of the work reported in this paper is experimental evidence of the relation between the asperity slopes and the wear of polymers.

Recent research (7,8) has shown that a single surface characterization parameter is insufficient for predicting the function of a surface. Often, two or more surface parameters are needed; the selection of the parameters being guided by physical models of the

¹ Based on a dissertation by J. H. Warren submitted to Virginia Polytechnic Institute and State University in partial fulfillment of requirements for the Degree of Doctor of Philosophy in Mechanical Engineering.

² Presently research engineer, DuPont Savannah River Laboratory, Aiken, South Carolina.

³ Numbers in parentheses refer to literature listed in References.

phenomena. Another portion of this paper presents wear data of polymers sliding on rough surfaces, and the surface parameters which correlate with the data.

EXPERIMENTAL

Wear experiments were performed on a pin-on-disk machine described in detail in (3,9). In one series of tests, the polymer pin was moved radially while the disk rotated creating a spiral track for 5 revolutions of the disk. In the other series of tests, a rectangular block was fastened to the turntable which was held stationary while the polymer pin was moved radially. This procedure created a straight line wear track.

For the wear experiments on the rotating disks, two polymer pin geometries were used. One geometry was a 7.9 mm long, 3.18 mm dia rod with a 20° half angle cone turned on one end. The other geometry was a truncated cone, formed by machining a 0.25 mm flat on the cone. For the experiments on the rectangular block, only conical pins were used.

Two polymers were chosen for the experiments on the rotating disks, PCTFE and PVC. The PCTFE was received in the form of 3.18 mm dia extruded rod. To remove the anisotropy of mechanical properties caused by the extrusion process, the rods were placed in quartz tubes, heated in a furnace to 218 C and held at that temperature for one half hour. The furnace was turned off and after the rods cooled down to 100 C over a one-hour period they were removed from the furnace. This heat treatment produced a structure that was 65 percent crystalline (3,10). The machining was done after heat treating. The PVC was received in the form of 6.36 mm dia rods which were machined to 3.18 mm dia and conical on one end. Tensile specimens were prepared by machining the 6.36 mm rod down to 3.18 mm dia over a 50.8 mm gauge length.

For the experiments on the rectangular block nylon 6/6 was tested in addition to PVC and PCTFE. The 3.18 mm dia nylon 6/6 was machined to a 7.9 mm length and conical on one end. Mechanical property data for all three polymers are given in Table 1.

The disks and rectangular blocks were made of mild steel and surface ground. The disks were ground with a radial lay so that the sliding direction was always perpendicular to the lay direction. The sliding direction on the rectangular block was also always perpendicular to the lay.

Table 1. Mechanical Property Data for Polymers

	PCTFE ¹ 25C	PVC ² 25C	Nylon 6/6 ³ Dry ⁴ Condi- tioned ⁵	
Tensile Strength (MN/m ²)	35.85	102.38	86.9	59.3
Elongation to Break (m/m)	1.25	0.263	0.90	2.40
Yield Point (MN/m ²)	36.54	136.86	-	-
Yield Strength (0.2% offset, MN/m ²)	23.10	103.42	86.9	59.3
Modulus of Elasticity (Tension, GN/m ²)	1.31	3.94	3.28	2.65
Energy to Rupture (Tension, MNm/m ³)	41.82 ⁶	24.82 ⁷	78.2 ⁸	142.3 ⁸

The experiments were run at an average sliding speed of 0.935 cm/sec. For the spiral tracks, the speed varied from 0.859 cm/sec at the inside radius to 1.01 cm/sec on the outside radius. The experiments were run in laboratory air at 24 C and 60 percent relative humidity. In addition to the different polymers and different pin geometries other experimental variables were the normal load and the surface roughness. The experimental variables are given in Table 2.

No wear measurements were made on the rectangular block. The blocks were photographed in the SEM. The photographs were used to measure the angle between the shear plane for the polymer and the plane of the surface. Wear measurements were made on the circular disks using neutron activation analysis, a technique which is described in detail elsewhere (3,12).

All surfaces were profiled with a stylus instrument moving perpendicular to the lay. Several surface characterization parameters were calculated from the digitized analog data. The digitized height data was also used to calculate some specialized parameters which related to the experimental conditions in these tests.

Table 2 Experimental Variables

Linear Wear Track (Rectangular Block)			
Polymers: PVC, PCTFE, nylon 6/6			
Normal Loads (N): 2.45, 9.8, 14.7			
Pin Geometry: Pointed cone			
R _a (μm): 0.32			
Spiral Wear Track (Circular Disks)			
Polymers:	PVC, PCTFE	PVC, PCTFE	
Normal Loads (N):	0.98, 1.96	1.96	
Pin Geometry:	Truncated Cone	Pointed Cone	
R _a (μm):	0.25-0.43	0.10, 0.34	

RESULTS

Angle Measurements on Linear Wear Tracks

Shear angle measurements were made for all nine combinations of polymers and loads listed in Table 3. The actual measurements on the photographs were corrected for the angle of tilt of the specimen surface with respect to the electron beam on the SEM. Fig. 1 is a typical SEM photo showing the shear angles that were measured. The average, minimum and maximum angles measured, the number of measurements, the standard deviation of the measurements are given in Table 3.

¹ Ref. (10).

² Average values from 4 stress-strain curves, 5 mm/min. cross head speed.

³ Ref. (11).

⁴ Dry as molded.

⁵ Conditioned to 50% R.H.

⁶ Estimated from a stress-strain curve reconstructed from above data.

⁷ Area under stress-strain curve.

⁸ Tensile strength times elongation to break.

A test (13) of multiple comparisons was made which showed that the average angles were significantly different from each other except for the angles for PVC and PCTFE at the low load. A one-way ANOVA test also showed that the angles measured for a given polymer were not significantly different at the different loads except for PVC. For this polymer the average angle for the lowest load was significantly different from the angle measured at the highest loads.

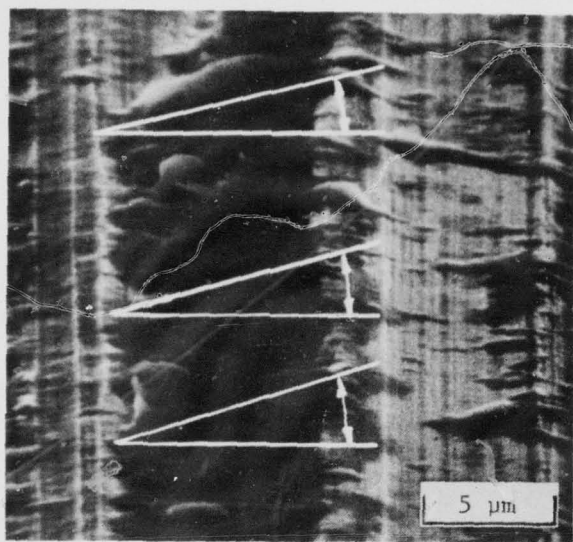


Fig. 1. Scanning electron photograph of nylon 6/6 transferred to a rough steel surface; full penetration. Typical sites where shear angles were measured are shown.

Table 3 Shear Angle Measurements

		Load, W (N)		
Polymer		2.45	9.8	14.7
PVC	n	99	84	106
	ϕ_l	2.12	3.59	2.64
	ϕ_h	11.9	10.9	9.81
	ϕ_s	19.9	24.2	34.7
	s	3.80	4.26	4.38
PCTFE	n	49	60	46
	ϕ_l	6.87	6.87	6.34
	ϕ_h	13.3	12.4	12.0
	ϕ_s	26.2	19.9	16.6
	s	3.49	2.52	2.67
Nylon 6/6	n	56	64	128
	ϕ_l	7.82	9.51	7.19
	ϕ_h	18.6	19.0	19.0
	ϕ_s	32.9	34.0	46.6
	s	4.98	5.06	5.55

Wear Measurements on the Spiral Tracks

The mass of polymer transferred to the disks is shown in Table 4. The percent error can be used to estimate the standard deviation of the transferred mass caused by the statistics of the decay process. The decay process can be described by a Poisson distribution, for which the mean and variance are equal. Hence the standard deviation

of the Poisson distribution is the square root of the mean value. The standard deviation for the mass transferred can be estimated by multiplying the percent error by the mass transferred divided by 100. The percent error increases as the amount of transfer decreases, a relation that limits the sensitivity of the wear measurement.

On disks 20, 31, 33, 11 and 22, the PCTFE experiments were run first. The subsequent PVC experiments were run at a different radii. Thus, the wear data were normalized by the length of the wear track so that direct comparisons could be made of wear at different radii. On disks 19 and 31 the PVC experiments were run first. Because PVC can be dissolved in chloroform, whereas PCTFE has no convenient solvents, the transferred PVC was dissolved off the disks and the subsequent PCTFE experiments were run at the same radii. Hence, direct comparisons can be made between polymer transfer at the same load on the same surface on disk 19, and at different loads on the same surface on disk 31.

Table 4 Mass of Polymer Transferred to Circular Disks

		Truncated Cone Mass (10^9 kg/m)	
Disk	Load (N)	PCTFE	PVC
18	1.96	---	7.16 (5.52) ¹
19	0.98	2.91 ^{*2} (6.79)	5.73 [*] (6.37)
20	0.98	0.46 (17.2)	0.96 (16.3)
31	1.96	0.89 (13.9)	1.08 [*] (14.4)
	0.98	0.70 [*] (14.2)	---
33	1.96	2.14 (8.0)	1.47 (13.5)
		Pointed Cone	
11	1.96	0.17 (32.0)	0.22 (22.3)
22	1.96	7.69 (4.38)	20.10 (3.32)

¹ Numbers in parentheses are percent error, PE.

² Starred values were run at same radii, on the same disk.

Surface Characterization

Surface profiles of all disks and one rectangular block were made and several surface statistics were calculated for each surface. These statistics are given in Table 5. The definitions of these parameters are given in Ref. 8 and 9. In addition to the parameters in Table 5, the power spectral density, auto correlation function and the bearing area curve were calculated for each surface. Finally, certain statistics, such as the mean absolute slope were calculated for only that portion of the profile which penetrated the polymer in the truncated cone experiments.

DISCUSSION

The loads on the pointed cones in the experiments run on the rectangular blocks were high enough to cause full penetration of the asperities into the polymer. Full penetration is defined as the penetration required to make the real and apparent areas

Table 5 Surface Statistical Parameters

	Disk					Rectangular Block			
Parameter	18	19	20	31	33	11	22		
R_a (μm)	0.26	0.41	0.40	0.25	0.43	0.10	0.34	0.32	0.82 ¹
RMS (μm)	0.35	0.70	0.51	0.31	0.54	0.14	0.47	0.43	0.88
Mean Absolute Slope	0.026	0.032	0.033	0.023	0.038	0.0072	0.023	0.032	0.052
Reciprocal Mean Peak Curvature (μm)	36.0	34.4	29.2	37.6	44.6	--	--	18.9	11.2
Peak-to-Valley Height (μm)	3.84	5.41	2.97	2.45	2.94	1.17	7.00	3.17	6.08

¹ All values in the table were obtained with a 762 μm waviness filter except the values on this column for which no filter was used.

approximately equal. The SEM photographs showed that the polymer sheared off at an angle to the horizontal plane. This angle is defined as the shear angle. The shear angles varied considerably as shown in Table 3 by the maximum and minimum shear angles measured and the standard deviations. However, the shear angles were independent of load for a given polymer. As the normal load is changed in full penetration, the real and apparent areas change to support the load - the load on each asperity will remain relatively constant. Hence, the forces causing shear at the asperity will be independent of the total normal load.

One purpose for the shear angle measurements was to determine if there was a minimum shear angle below which polymer was not removed. If an asperity removes polymer the shear angle for the polymer must be less than the slope angle for the asperity. Hence, with each shear angle measured there is a corresponding asperity slope angle which is larger than the shear angle. If a limiting shear angle were observed, it would imply that there was a larger, limiting asperity slope angle.

The data in Table 3 shows that the minimum and mean shear angles are lowest for PVC, intermediate for PCTFE, and maximum for nylon 6/6. Referring to Table 1, the energy-to-rupture is lowest for PVC, intermediate for PCTFE and highest for nylon 6/6. Hence, the minimum and mean shear angles correlated positively with the energy-to-rupture for the polymers.

Consider now two polymers with different energies-to-rupture sliding on the same rough surface with a normal load sufficient to cause full penetration. The above correlation suggests that the polymer with the lower energy to rupture will have a lower minimum shear angle. The lower minimum shear angle is associated with a lower minimum asperity slope. Hence, more asperities will be removing the polymer with the lower energy to rupture and the wear of this polymer will be greater than that for the polymer with the higher energy to rupture. This conclusion agrees with Ratner's data (4) and with the data in Table 4 for the pointed cone.

In Table 4, the data for the pointed cone represents wear when the normal load causes full penetration. On each disk, the PVC wore more than the PCTFE; for disk 11, the PVC wear was 1.3 times that for PCTFE, on disk 22, the PVC wear was 2.6 times

that for PCTFE. The ratio of the energy-to-rupture of PCTFE to that for PVC from Table 1 is 1.68. Hence, the inverse of the energy to rupture is positively correlated with the full-penetration wear for these polymers.

Table 4 also shows that the wear on disk 22 was more than an order of magnitude greater than that for disk 11. The surface topography parameters in Table 5 show that disk 22 had higher R_a , RMS, mean absolute slope, and peak-to-valley height than disk 11. The higher average slope for disk 22 implies that there were more asperities with slopes above the minimum slope angle. Hence, more asperities were removing polymer on disk 22. The greater height of the asperities on disk 22 results in more polymer removed at each asperity than for disk 11.

The truncated cone experiments were designed so that the real area of contact would be less than the apparent area of contact, a condition which is called partial penetration in this paper. ²The apparent area for all experiments was 0.25 mm^2 . The real area was estimated from $A_r = W/3Y$ where W is the normal load and Y is the yield strength for the polymer. Table 6 gives the ratio of the real to the apparent area for the loads and polymers.

The disks were selected for the truncated cone experiments on the basis of an R_a value measured by surface analyzer designed for production or quality control use. The disks selected had approximately the same R_a values. However, when measured by a more sensitive research surface analyzer a variation in R_a values for the disks was found as well as variations in several other surface characterization parameters. Therefore, the wear measured was a function of the polymer, load, and the surface topography.

The effect of the polymer on wear is shown on disks 19, 20, 31 and 33 in Table 4. For disks 19, 20, and 31 the ratios of PVC wear to PCTFE wear were 1.97, 2.11, and 1.20, respectively. The inverse of the energy-to-rupture would predict that PVC would wear 1.68 times that for PCTFE. However, the PVC wear on disk 33 is less than that for PCTFE. Thus, energy to rupture, by itself, does not appear to be an accurate predictor of the wear of these polymers for partial penetration. However, by combining energy-to-rupture and the associated shear angle for polymers with surface topography information, greater insight into the variations in measured wear can be obtained.

For these experiments with the truncated cones partial penetration occurs. Therefore, it is only the upper portion of the profile which is in contact with the polymer. Fig. 2 shows the bearing area curve for the upper portion of the profile for all five disks. The penetration depth is the distance that the highest asperity must penetrate the polymer in order to support the normal load. The values of bearing area from Table 6 are plotted as vertical lines on the graph. The intersection of the vertical lines with the bearing area curves defines the depth of penetration for each polymer, load, and disk combination tested. The average slope of the asperities in contact was calculated for each experiment. All these data are summarized in Table 7.

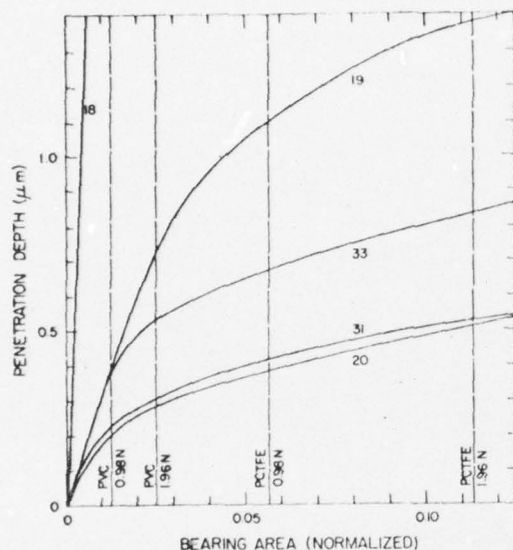


Fig. 2. Penetration depth as a function of bearing area for several disk, polymer, and load combinations. Numbers on curves are disk numbers.

Table 6

Ratio of Real to Apparent Area of Contact

Polymer	Load (N)	
	0.98	1.96
PVC	0.0126	0.0252
PCTFE	0.0566	0.113

The wear is plotted as a function of the depth of penetration in Fig. 3. While there is considerable scatter in the data, the wear of PCTFE at a given depth is less than that for PVC. Thus, the penetration depth is a parameter which can discriminate between the wear of PVC and PCTFE. The shear angle measurements in Table 3 support the results shown in Fig. 3. If PVC and PCTFE are penetrated to the same depth by a surface, more asperities will remove PVC than PCTFE because the minimum shear angle for PVC was observed to be less than that for PCTFE. In addition, because the mean shear angle for PVC is less than that for PCTFE, more PVC will be removed by a given asperity than PCTFE.

Table 7 Wear and Profile Data

Disk	Load (N)	Polymer	Depth (μm)	Slope	Wear (10^9 kg/m)
18	1.96	PVC	1.95	0.084	7.16
19	0.98	PCTFE	1.08	0.069	2.91
19	0.98	PVC	0.40	0.060	5.73
20	0.98	PCTFE	0.38	0.052	0.46
20	0.98	PVC	0.20	0.078	0.96
31	1.96	PCTFE	0.52	0.039	0.89
31	1.96	PVC	0.31	0.047	1.08
31	0.98	PCTFE	0.42	-	0.70
33	1.96	PCTFE	0.83	0.051	2.14
33	1.96	PVC	0.52	0.071	1.47

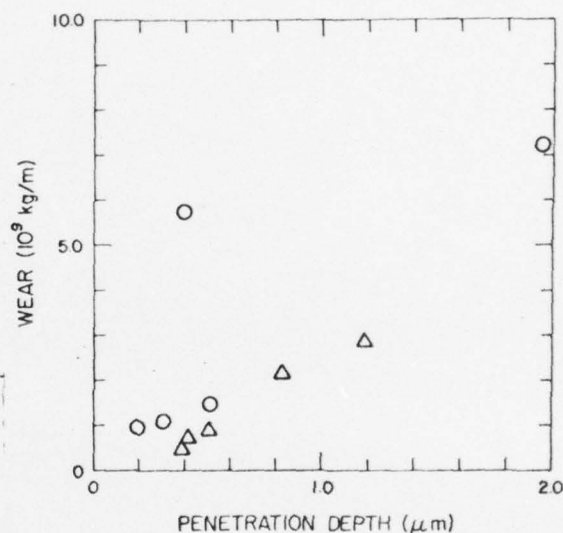


Fig. 3. Polymer wear as a function of penetration depth. ○- PVC, △- PCTFE.

The penetration depth is a parameter which is a function of the flow pressure of the polymer and the bearing area curve for the surface. Hence, it is a parameter which cannot be directly measured but must be calculated. The flow pressure has been estimated in these calculations by $3Y$. However, since Y is a function of strain rate, the appropriate value of Y to use in estimating flow pressure will depend on knowledge of the strain rates expected in sliding and the wear process. Hence, one reason for slow sliding speed in these experiments was to try to keep strain rates low and comparable to those used in measuring mechanical properties.

When the real area has been calculated from $A_r = W/3Y$, this area must be related to the bearing area curve. In this paper, it has been assumed that the real area is that formed by the intersection of a plane parallel to the mean plane of the profile with the solid portion of the surface. This assumption is valid for normal loads only. However, when tangential loads are applied at sliding commences, most of the normal load supplied by the trailing flanks of the asperities will be transferred to the leading

edge. Hence, the penetration depth would be larger than predicted in these calculations.

An estimate of the upper limit for the penetration depth during sliding can be made by assuming that the normal load is supported only on the leading edges of the asperities. Hence, to estimate the penetration depth the value of the bearing area curve equal to twice the real area would be used. However, the effect of this penetration depth on the data in Fig. 3 would be to move all data points to the right. The conclusions drawn from Fig. 3 would remain unchanged.

The penetration depth is a parameter which is defined by the extreme peak of the profile. Profile statistics are obtained from only a small sample of the surface on which sliding occurs. It is generally assumed that the sample selected is representative of the entire surface. However, if the sample does not include the highest peaks in the surface, a parameter such as the penetration depth will be estimated to be smaller than its maximum possible value. Hence, the wear predicted by this depth will be smaller than actually measured. It might be argued that the omission of the highest peak from the profile sample would have a small effect on the overall wear predicted because the peak only occurs once per disk revolution. However, it can easily be shown that for similarly shaped asperities, the volume removed varies as the square of the penetration depth. Thus, 10 asperities penetrating 0.1 μm will remove one-tenth the amount of material as one asperity penetrating 1 μm .

It should be noted that the wear data cannot be correlated with anyone of the following parameters: the energy-to-rupture for the polymers, normal loads, average slopes, or the standard roughness parameters such as R_a or RMS. The polymer properties interact with the surface roughness in the wear process. Both polymer properties and surface roughness characteristics are combined in a parameter such as the penetration depth. The effect of the interaction of surface characteristics and polymer properties on wear was also observed in multiple pass experiments (3).

Surface profile instruments have electronic filters which remove the long wavelengths (waviness) from the surface profile information allowing only the higher frequency components to be passed. The data for the rectangular block in Table 5 shows the difference in profile statistics with and without a 762 μm waviness filter. It is obvious that the non-filter statistics are significantly larger. Hence, when obtaining profile statistics for wear prediction, it is important that the selection of a waviness filter be dictated by the geometry of the sliding members. One general guideline would be to include wavelengths equal to or less than the largest dimension of the apparent area of contact in the sliding direction.

CONCLUSIONS

When polymers are loaded against rough hard surfaces in a condition of full penetration and slid along the surface, the polymer shears off at an angle to the horizontal surface. The shear angles are significantly different for PVC, PCTFE and nylon 6/6 and the shear angles correlate with the energy-to-rupture for the polymer. The shear angle data also indicates that there are minimum shear angles for the polymers which also correlate with energy-to-rupture for the polymers. Hence, if

different polymers are slid on the same surface, more asperities will remove the polymer with the lowest energy-to-rupture. Also, because the lower shear angle is associated with the lower energy-to-rupture polymers, more of the lower energy-to-rupture polymer will be transferred per asperity.

For polymers sliding on rough-hard surfaces under partial penetration, wear of different polymers can be discriminated by the depth of penetration parameter. This parameter is a function of the polymer mechanical properties (yield strength) and the surface profile characteristics (bearing area curve). This conclusion is based on the data from only two polymers. Thus, considerably more test data is needed to explore the utility of penetration depth for wear prediction in partial penetration experiments.

Surface profile statistics are vital in the prediction of wear of polymers on hard, rough surfaces. However, the use of waviness filters must be selected in consideration of the apparent area of contact. The statistics calculated must be applicable to the portion of the profile in contact with the polymer. Hence, statistics based on the total profile can be meaningless in sliding where partial penetration is occurring.

ACKNOWLEDGEMENTS

This work was supported by a grant from the Army Research Office, Research Triangle Park, North Carolina as a portion of a study on the wear of polymers by the mechanism of transferred films. The authors gratefully acknowledge the assistance of H. T. McAdams of Calspan Corp., Buffalo, New York in the surface analysis of the specimens. The cooperation of the personnel of the Neutron Activation Analyses Laboratory, V.P.I. & S.U. in providing space for the wear apparatus and analysis of the wear data is appreciated.

REFERENCES

1. Briscoe, B. J., Pooley, C. M., and Tabor, D., "The Friction and Transfer of Some Polymers in Unlubricated Sliding," in Lee, L. H., ed., *Advances in Polymer Friction and Wear*, Plenum Press, New York, 1974, pp. 191-204.
2. Pooley, C. M., and Tabor, D., "Friction and Molecular Structure: The Behavior of Some Thermoplastics," *Proc. Roy. Soc., London, Series A*, Vol. 329, 1972, pp. 251-274.
3. Eiss, N. S., Jr., Warren, J. H., and Quinn, T.F.J., "On the Influence of the Degree of Crystallinity of PCTFE on its Transfer to Steel Surfaces of Different Roughnesses," to be presented at the Leeds-Lyon Symposium on Friction and Wear of Non-Metallic Materials, 7-10 September 1976, Leeds, England.
4. Ratner, S. B. et al., "Connection Between Wear Resistance of Plastics and Other Mechanical Properties," in James, D. I., ed., *Abrasion of Rubber*, McLaren & Sons, London, 1967, p. 145.
5. Lancaster, J. K., "Basic Mechanisms of Friction and Wear of Polymers," *Plastics and Polymers*, Vol. 41, Dec. 1973, pp. 297-306.
6. Rabinowicz, E., *Friction and Wear of Materials*, John Wiley & Sons, New York, 1965, p. 168.

7. Eiss, N. S., Jr., and Warren, J. H., "Current Advances in Surface Characterization," to be presented at the 2nd ASME Design Technology Transfer Conference, Montreal, 27-30 September 1976.
8. Thomas, T. R., "Recent Advances in the Measurement and Analysis of Surface Microgeometry," Wear, Vol. 33, 1975, pp. 205-233.
9. Eiss, N. S., Jr., and Warren, J. H., "The Effect of Surface Finish on the Friction and Wear of PCTFE Plastic on Mild Steel," Soc. Manu. Engrg. Paper No. IQ75-125, April 1975.
10. "Physical Properties of KEL-F 81 Plastic," Tech. Info. Bull., 3M Company, August 1, 1961.
11. "Materials Selector 75," Materials Engineering, Vol. 80, No. 4, September 1974, p. 186.
12. Eiss, N. S., Jr., Doolittle, S. D., and Warren, J. H., "An Application of Neutron Activation Analyses to the Measurement of the Wear of Polymers," Wear, Vol. 38, No. 1, 1976, pp. 129-143.
13. Kramer, C. Y., "Extension of Multiple Range Tests to Group Means with Unequal Numbers of Replications," Biometrics, Vol. 12, 1956, pp. 307-310.

APPENDIX 4

Full Penetration Wear Model

from a Ph.D. dissertation

THE PREDICTION OF POLYMER WEAR USING
POLYMER MECHANICAL PROPERTIES AND SURFACE
CHARACTERIZATION PARAMETERS

by

Jeffery H. Warren

Virginia Polytechnic Institute and State University
Blacksburg, Virginia

August 1976

APPENDIX 4

Full Penetration Wear Model

4.1 Single Point Orthogonal Cutting Theory

The consideration and determination of factors important in a wear model, consistent with the wear and shear angle data already presented, were the major efforts of this research. From the SEM observations of wear tracks, polymer deposits were seen to be distributed in discrete sites rather than continuous films. It was apparent that some of the steel asperities were removing material and some were not. It was also apparent, due to the differences in the amount of polymer deposited at these discrete sites, that some asperities were removing more material than others. Thus two important questions must be answered in order to construct a wear model:

- 1) Which of the steel asperities are going to remove material?
- 2) How much material will they remove?

It is noted that the process of the cutting or machining of metals is related to the polymer wear mechanism, where the cutting tool and the steel asperity are analagous. Therefore, in order to answer the above questions and develop a wear model, a modification to orthogonal cutting theory was made. Before discussing the model, a brief review of orthogonal cutting theory must be presented.

Orthogonal cutting occurs when the cutting edge of a tool is a straight line perpendicular to the direction of motion of the tool [1].

The forward face of the tool is usually considered to be a plane surface and the angle which this plane surface makes with the normal to the newly formed metal surface is called the rake angle (α). All of the forces of an orthogonal cutting system lie in a plane and may be represented as shown in Fig. 1. This figure illustrates a positive rake angle, but the mathematics applies to both positive and negative rake angles if the appropriate sign is attached to α .

The tool is driven through the work-piece with a horizontal force F_c and a vertical force F_v giving a resultant force vector R , which forms the diameter of the force circle. The chip in escaping exerts a friction force F along the tool surface and a normal force N perpendicular to the surface.

The relative magnitudes of F and N are determined by the coefficient of friction μ according to the usual relation

$$\mu = \tan \tau = F/N \quad (2)$$

The forces on the shear plane consist of a compressive force F_N and a shearing force F_S . The shear plane of area A_S is the plane in which the shear stress

$$S_S = F_S / A_S \quad (3)$$

is a maximum.

The model is based on the assumption that all material in the path of the tool is removed as a chip. The work-piece shears along a narrow zone which is the plane of maximum stress leading from the tip of the tool to the surface of the work-piece and forming an angle ϕ with the direction of tool travel. Assuming a constant shear strength for the

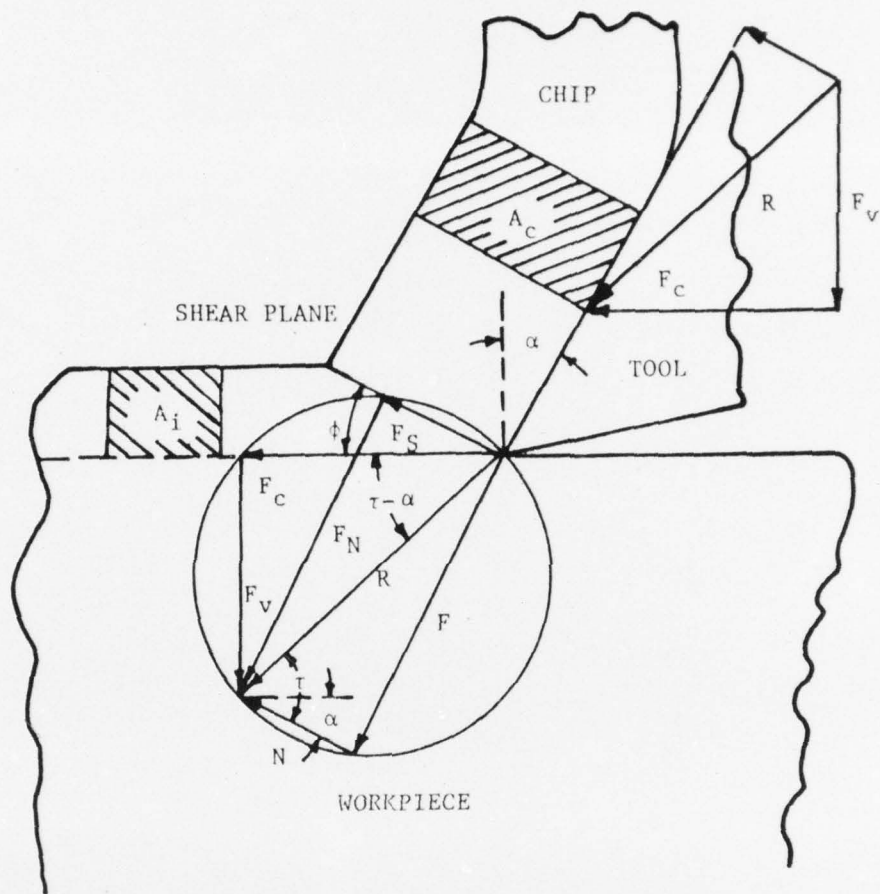


Figure 1. Force Diagram Showing Geometric Relationships Between Forces At Tool Point When No Built-Up Edge Exists [1].

material being cut, invariant with respect to ϕ and solving for the plane in which the shear stress is a maximum, Ernst and Merchant [2] defined the location of the shear plane ϕ as

$$\phi = 45^\circ + \frac{\alpha}{2} - \frac{\tau}{2} \quad (3)$$

Therefore, the shear plane angle is defined by the rake angle and the coefficient of friction between the tool and chip. The shear stress on the shear plane has a value equal to

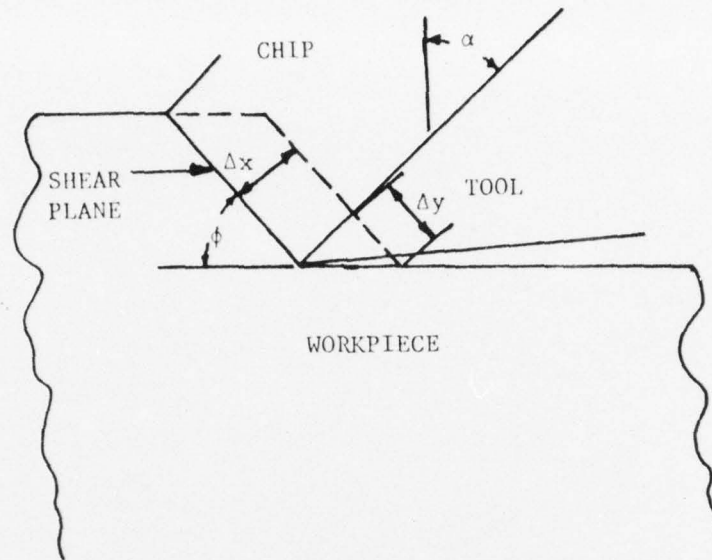
$$S_S = \frac{R \cos (\phi + \tau - \alpha)}{A_i / \sin \phi} \quad (4)$$

Kobayashi and Thomsen [3] defined the shear strain (γ_S) in metal cutting as shown in Fig. 2a. In the case shown

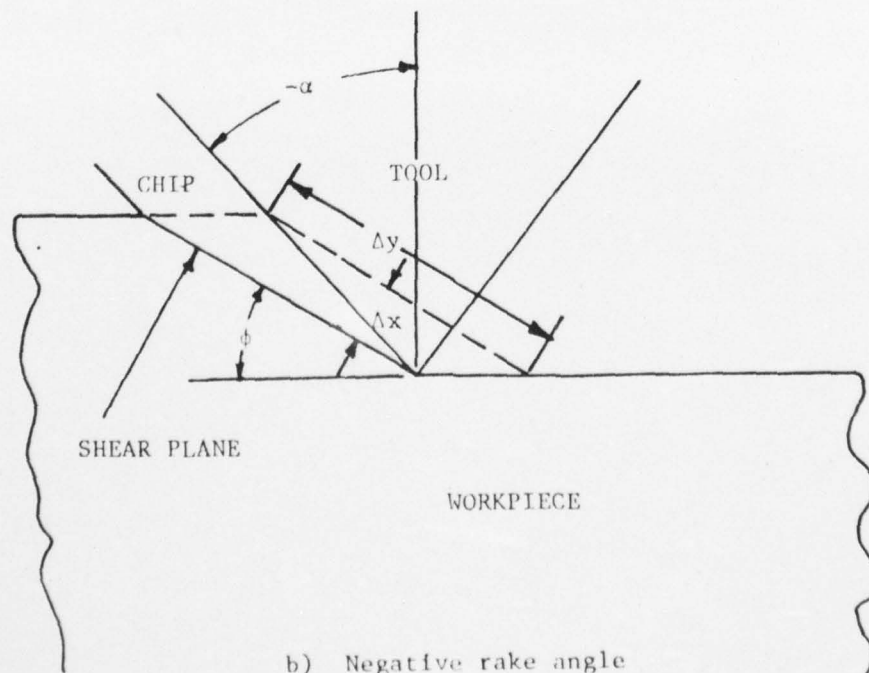
$$\gamma_S = \lim_{\Delta x \rightarrow 0} \frac{\Delta y}{\Delta x} = \cot (\phi) + \tan (\phi - \alpha). \quad (5)$$

The shear strain defined by Eq. 5 is a measure of large plastic shear deformation and also holds for negative rake angles as shown in Fig. 2b.

In reference 4, Merchant found that the constant shear strength assumption was a poor approximation in the case of the cutting of a polycrystalline metal. The reason for this is that the shear strength is influenced by a number of different quantities. The most important are temperature, rate of shear, shearing strain (plastic) and the stress acting normal to the plane of shear. Merchant concluded that of the above quantities, the normal or compressive stress existing on the potential shear planes ahead of the cutting edge was the only one which was active in influencing the shear strength when the metal was merely stressed and had not yet started to undergo plastic strain.



a) Positive rake angle



b) Negative rake angle

Figure 2. Shearing Process on the shear plane [3].

He concluded that temperature, rate of shear, and shearing strain should all be secondary in their influence on the shear angle, compared to the compressive stress on the shear plane.

According to Merchant, the shear strength of a polycrystalline metal had been quite extensively investigated and for conditions closely duplicating those in metal cutting the relationship between shear strength and normal stress was approximately linear. Therefore, the shear strength of the metal (S'_S) was defined as

$$S'_S = S'_O + kS_N \quad (6)$$

where S'_O is the shear strength of the metal under zero compressive stress, S_N is the normal stress, and k is the slope of the shear strength versus compressive stress curve. S'_O is approximately equal to one-half the tensile strength of the metal at high values of strain.

Using Eq. 6, Merchant again solved for the plane of maximum shear stress. In this case Eq. 3 became

$$\phi = \frac{C + \alpha - \tau}{2} \quad (7)$$

where

$$C = \text{arccot}(k) \quad (8)$$

The shear stress on the shear plane is then equal to

$$S_S = \frac{F_c}{A_f} \frac{1}{\cot \phi + \tan (C - \phi)} \quad (9)$$

4.2 Full Penetration Model

Figure 3 illustrates the forces acting on a single steel asperity with full penetration under the application of normal (W) and tangential (F) loads. Lines BC and CD denote the steel asperity. Under static conditions the polymer and steel make contact on the surface ABCDE. When a tangential force (F) is applied to the asperity as shown in Fig. 3, the polymer no longer contacts the steel along CDE, where E is determined by the viscoelastic properties of the polymer, the rate of tangential loading and the rate of wear. In the orthogonal cutting theory, as previously discussed, shear occurs along a shear plane AC making an angle ϕ with the horizontal. The chip is free to move along the steel surface BC. However, in this single asperity wear model, the "chip", or polymer deposit, is not free to move along the steel asperity face due to the steel surface AB. Therefore, there can be no friction force between the steel asperity and the polymer deposit along BC and hence τ must equal zero. The only way τ can equal zero is for the resultant R to be perpendicular to the cutting side of the steel asperity BC. The amount of normal load (W) supported by the asperity is

$$W = \frac{A_i \cdot \tan(-\alpha)}{A_r} \cdot W_t \quad (10)$$

where BC is the length of side BC, A_i is the cross sectional area of the polymer as shown in Fig. 3, W_t is the total normal load and A_r is the real area of contact of the entire polymer pin.

Knowing the direction of R , the magnitude and direction of W , and

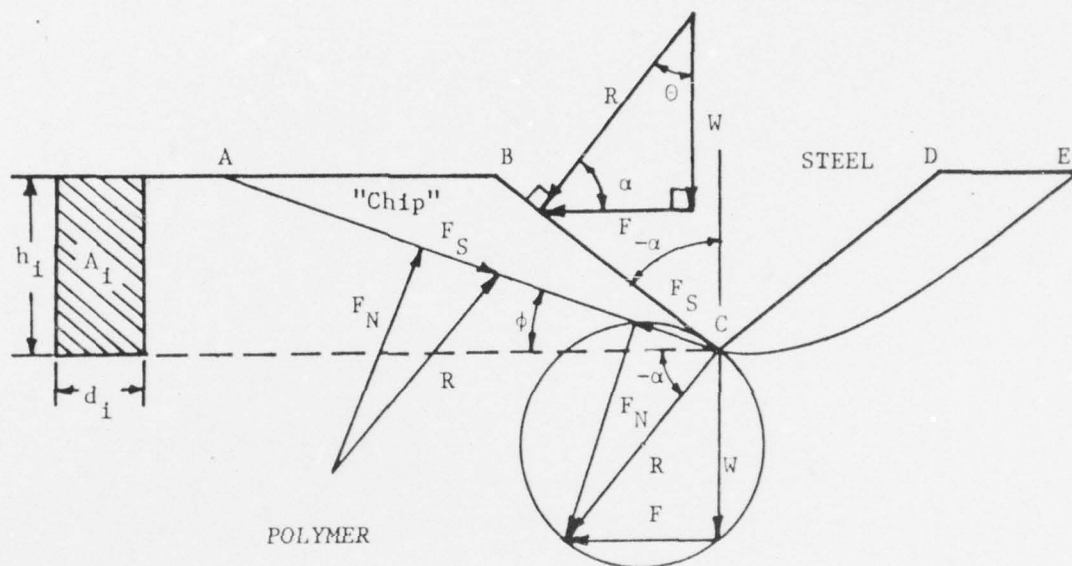


Figure 3. Forces acting on a single steel asperity.

AD-A037 104

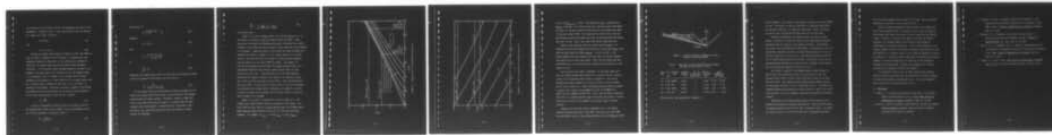
VIRGINIA POLYTECHNIC INST AND STATE UNIV BLACKSBURG --ETC F/G 11/9
THE WEAR OF POLYMERS BY TRANSFERRED FILMS.(U)
JAN 77 N S EISS

DA-ARO-D-31-124-73-G170
NL

UNCLASSIFIED

ARO-11229.3-E

2 OF 2
AD
A037104



END

DATE
FILMED
4-77

037

the direction of the friction force F , the magnitude of R and F can be determined. As shown in Fig. 3, the angle between R and W is defined as θ where, $\theta - \alpha = 90^\circ$. Therefore

$$R = W / \cos \theta \quad (11)$$

and

$$F = W \cdot \tan \theta. \quad (12)$$

Because the average shear angles for Nylon 6-6, PVC, and PCTFE, as given in Table 3, Appendix 4 were different, it appeared that some mechanical property or properties of the polymers must influence ϕ . Therefore, the polymer wear model must include polymer mechanical properties. If the constant shear strength assumption is made for the polymers, the shear angle ϕ is a function of only the asperity angle ($-\alpha$) according to Eq. 3. However, if one assumes that the shear strength of the polymer is a linear function of the normal stress, then Eq. 7 predicts that ϕ changes not only with $-\alpha$ but also with k , a property of the polymer. Therefore, the shear strength of the polymer was assumed to be a linear function of the normal load as described in Eq. 6 for the wear model. With $\tau=0$, Eq. 7 became

$$\phi = \frac{C + \alpha}{2} \quad (13)$$

In order to determine the shear stress on this plane, which is the maximum shear stress in the polymer, F_c / A_1 was determined so that Eq. 9 can be evaluated. Referring to Fig. 3

$$F_c = \frac{W}{\tan (-\alpha)} \quad (14)$$

and from Eq. 10

$$W = \frac{A_i \tan(-\alpha)}{A_r} W_t \quad (15)$$

Assuming

$$W_t = A_r p_m \quad (16)$$

then

$$F_c = \frac{A_i \tan(-\alpha) A_r p_m}{A_r \tan(-\alpha)} \quad (17)$$

or

$$\frac{F_c}{A_i} = p_m \quad (18)$$

Therefore, the maximum shear stress in the polymer occurs along an angle ϕ with the direction of horizontal pin travel and is

$$S_S = \frac{p_m}{\cot \phi + \tan(C-\phi)} \quad (19)$$

It was assumed that the relative motion between the slider and the surface will produce sufficient strain to cause rupture if the maximum stress exceeds the shear strength. Therefore, rupture or shear will occur if the shear stress (S_S) is equal to or greater than the shear strength (S'_S) of the polymer. Substituting Eq. 13 into Eq. 9 and setting $S_S \leq S'_S$, then those asperities that have values of α which satisfy the following

$$\frac{S'_S}{p_m} < \frac{1}{\cot \frac{(C+\alpha)}{2} + \tan \frac{(C-\alpha)}{2}} \quad (20)$$

will produce wear.

Figure 4 is a plot of S'_S/p_m versus α for various values of k . On this graph, the values of S'_S/p_m are shown for PVC and PCTFE. These values were calculated by assuming S'_S was equal to one half the tensile strength of the polymer and p_m was equal to three times the yield strength of the polymer. Tabulated values of the tensile and yield strength were obtained from Table 1, Appendix 3. For a given value of k , one notes in Fig. 4 that PVC will shear for values of α which are more negative than the values of α for which PCTFE will shear. For example, if $k=0$ for both polymers, PVC will shear for angles ϕ greater than -53.5 deg whereas PCTFE must have asperity angles greater than -35.2 deg before shear will occur. This means that if $k=0$ for both polymers, asperities with angles α between -53.5 deg and -35.2 deg will produce wear on PVC and will not produce wear on PCTFE. Thus, PVC should wear more than PCTFE. It should also be noted in Fig. 4 that as k increases, the asperities must become sharper (α becomes less negative) in order to produce stresses in the polymer that are large enough to exceed the shear strength of the polymer.

Figure 5 is a plot of ϕ versus k for various values of α . The average shear angles measured from the profiles are also shown. One notes from this plot that for a given asperity angle, the average shear angles measured imply different values of k for the three different polymers. For example, if $\alpha_{avg} = -50$ deg, $k_{PVC} = 0.328$, $k_{PCTFE} =$

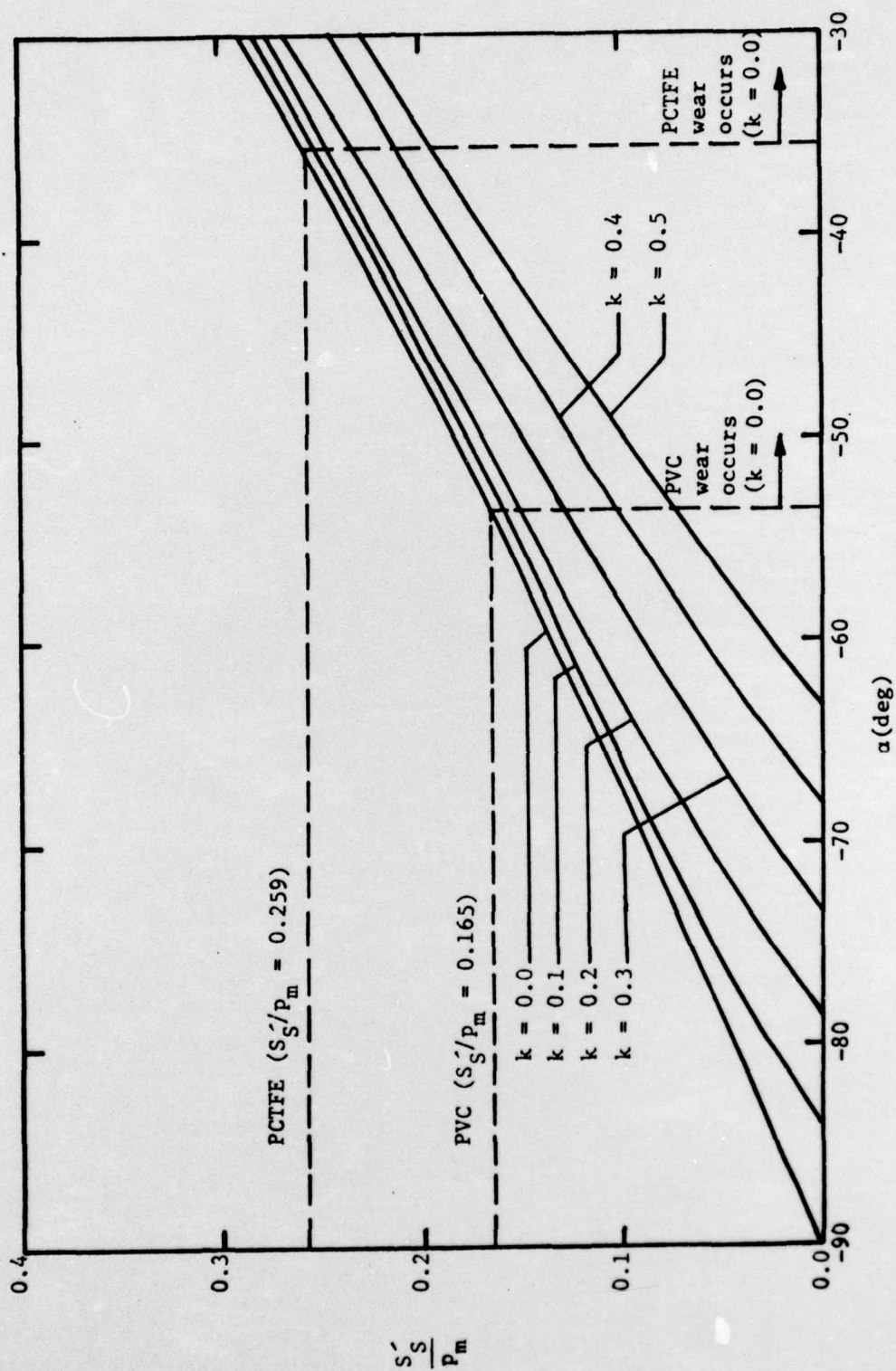


Figure 4. S'_S/p_m versus α for different values of k .

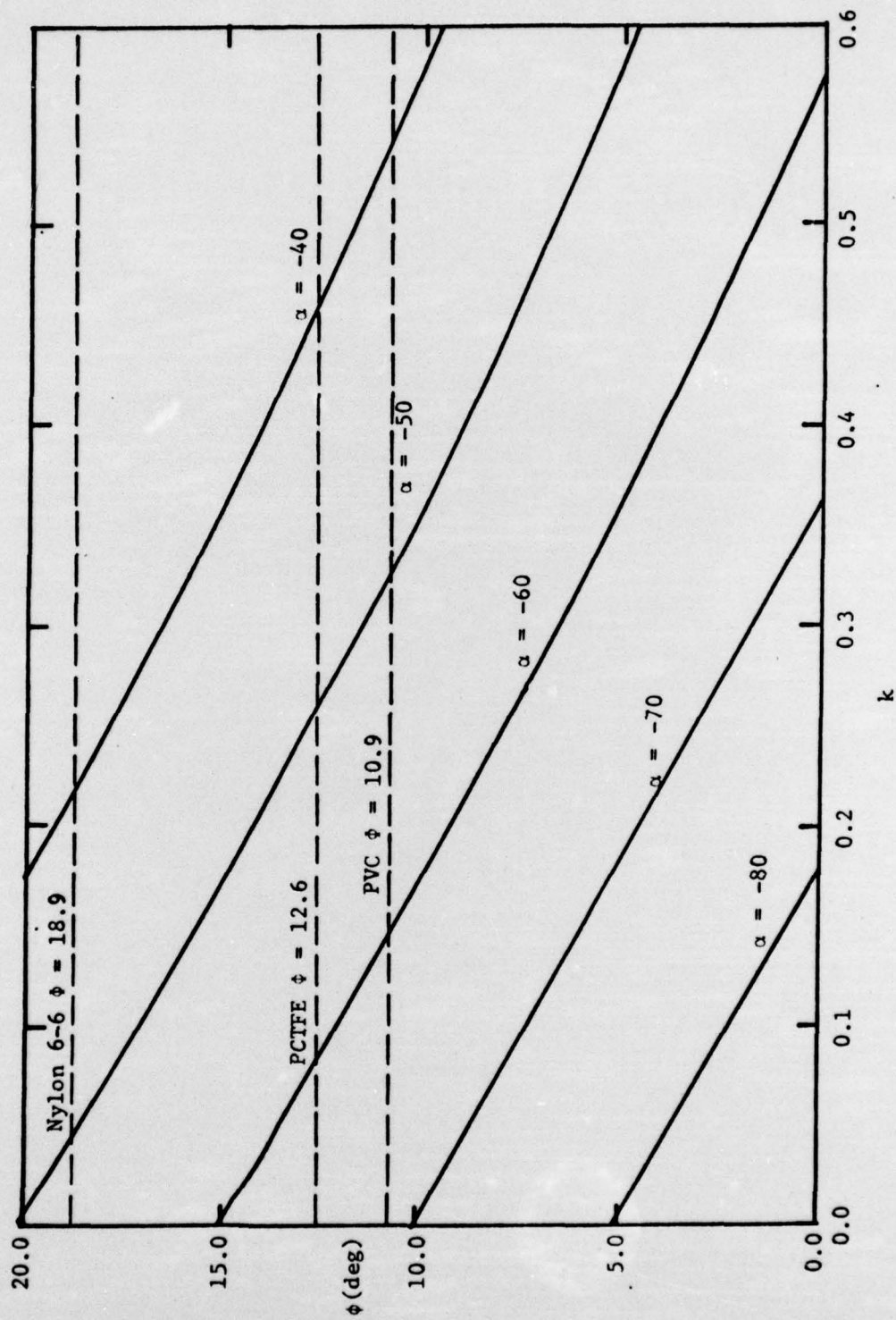


Figure 5 . Plot of ϕ versus k for various values of α .

0.264, and $k_{\text{Nylon 6-6}} = 0.040$. This shows that k_{PVC} is greater than k_{PCTFE} . From Fig. 4 for these values of k , asperities with rake angles less than -46 deg will remove PVC and those with rake angles less than -33 deg will remove PCTFE. For sliding on the same surface there are more asperities with rake angles less than -46 deg than with rake angles less than -36 deg. Hence, more asperities should remove more PVC.

Figure 5 also indicates that for a given asperity angle α , if PCTFE and PVC are being removed, PVC will have a shear angle (ϕ_{PVC}) less than the shear angle for PCTFE (ϕ_{PCTFE}). As seen in Fig. 6, the volume removed by a given asperity per unit depth is the area between the profile and the shear plane angle. Thus, PVC will again wear more than PCTFE with the cross hatched area indicating the difference in the amounts of wear.

One also notes from Table 3, Appendix 3 on the shear angle data that the minimum average shear angles also correlate with the energy to rupture of the polymers given in Table 1, Appendix 3. The overall minimum shear angle averages are 2.8 deg for PVC, 6.7 deg for PCTFE, and 8.2 deg for Nylon 6-6. These correlated positively with the energy to rupture (ER) values of 24.82 MNm/m^3 for PVC, 41.82 MNm/m^3 for PCTFE, and 142.3 MNm/m^3 for Nylon 6-6. Thus, this was another indicator that there is a minimum asperity angle below which the product of stress times strain attained in the polymer is not high enough to produce fracture.

Comparing the wear and surface topography data to this model, several conclusions are made. From Table 1 PVC wore more than PCTFE for both disks 11 and 22, correlating positively with the S'_s/p_m and $1/ER$

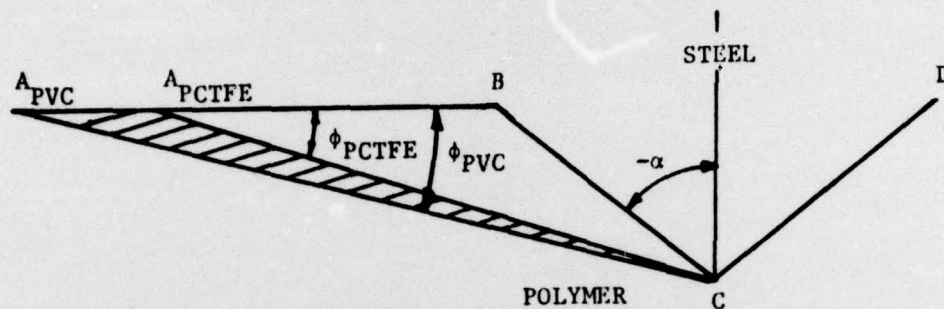


Figure 6. Volume of material removed by a given asperity for PVC and PCTFE.

Table 1. Wear Data for PVC and PCTFE Conical Polymer Pins Run on Steel Disks 11 and 12.

Disk No.	Load (N)	Polymer Pin	Average Radius (m)	No. of Revolutions Spiral Path	Distance Travelled (m)	Mass Transferred (10^9 Kg/m)
11	1.96	PCTFE	0.0143	5	0.4587	$0.1711 \pm 32.0\%^1$
11	1.96	PVC	0.0167	5	0.5244	$0.226 \pm 22.3\%$
22	1.96	PCTFE	0.0143	5	0.4587	$7.69 \pm 4.38\%$
22	1.96	PVC	0.0167	5	0.5244	$20.10 \pm 3.32\%$

¹Percent Error, see Nomenclature, Appendix 3.

of the polymers. The inverse of the energy to rupture for PVC and PCTFE is 1.68. From Table 1 on disk 11, PVC wore 1.3 times more than PCTFE and on disk 22 PVC wore 2.6 times more than PCTFE. Thus, the energy to rupture ratio was between the wear ratios for the two disks.

Comparing the wear data for LDPE with that for PVC and PCTFE (Table 2, Section 3.1) shows that three of four comparisons correlated positively with the inverse of the energy to rupture. The LDPE wear was greater than the PCTFE wear on both disks. The quantity on the 0.10 μm disk was larger by a factor of 5.46 and the quantity on the 0.34 μm disk was larger by a factor of 1.12. The energy-to-rupture of the PVC is 2.57 times greater than that of the PE. The PE wear on the 0.10 μm disk was greater than PVC by a factor of 4.22. However, the PE wear on the 0.34 μm disk was smaller by a factor of 2.34.

From Table 5, Appendix 3 the maximum peak-to-valley height for disk 22 was 7.00 μm whereas for disk 11 it was only 1.17 μm . The average profile slope for disk 22 was 0.0234 and on disk 11 the slope was only 0.0072. This implied sharper asperities and higher stresses in the polymer for disk 22 than 11, according to Fig. 4. The RMS and R_a roughness measures were greater for disk 22 than 11. Hence, all of the above measures of surface roughness correlated positively with the wear observed.

Comparison of the measured shear angles with the slopes of the asperities revealed the following inconsistency. From the profile data, the maximum asperity slope was 24.5 deg. According to Fig. 4, in order for shear and wear to occur for PVC with $k=0$, the maximum base angle

$(90 + \alpha)$ must be greater than or equal to 36.5 deg. Hence, the model predicted no wear when, in fact, wear did occur.

There are several assumptions that are made in the model which must be investigated further. One notes in Fig. 4 that if S'_S/p_m for each polymer were lower, wear would occur for asperities with smaller slopes. Therefore, the value of S'_S equal to one-half the tensile strength of the polymer might be too large and hence should be investigated for varying strain rates. Also the flow pressure of the polymer probably varies as a function of asperity angle and strain rate and might not be a constant equal to $3Y$ as shown and assumed for metals in reference 6. Because the shear angle data is different for different polymers, the shear strength must be a function of the compressive strength on the shear plane. However, the assumption of a linear relation (Eq. 6) should be verified for polymers.

In reference 5, Rao, et al. ran some cutting tests on Delrin and Zytel plastics and found that the coefficient of friction between the tool and the chip was approximately zero. Thus, the assumption that $\tau=0$ when the chip cannot move is correct.

4.3 References

1. Mohun, W. A. "Grinding with Abrasive Disks, Part 3 - Attritious Camber, Glazing and Rate of Cut," Trans. ASME, Journal of Engineering for Industry, November, 1962, pp. 451-465.
2. Ernst, H. and M. E. Merchant, "Chip Formation, Friction and Finish," Surface Treatment of Metals, American Society for Metals, Cleveland, Ohio, 1941, pp. 299-378.

3. Kobayashi, S. and E. G. Thomsen, "Metal Cutting Analysis -1, Re-Evaluation and New Method of Presentation of Theories," Trans. ASME, Series B, Journal of Engineering for Industry, February, 1962, pp. 63-70.
4. Merchant, M. E., "Mechanics of the Metal Cutting Process. II. Plasticity Conditions in Orthogonal Cutting," Journal of Applied Physics, 16, June, 1945, pp. 318-324.
5. Rao, U. M., J. D. Cumming, and E. G. Thomsen, "Some Observations on the Mechanics of Orthogonal Cutting of Delrin and Zytel Plastics," Trans. ASME, Journal of Engineering for Industry, 86, May 2, 1964, pp. 117-121.
6. Bowden, F. P. and D. Tabor, The Friction and Lubrication of Solids, Part I, Oxford U. Press, Ely House, London, 1950, pp. 10-14.

FILM
4

